ELSEVIER

Contents lists available at ScienceDirect

Chemical Geology

journal homepage: www.elsevier.com/locate/chemgeo





Investigating the influence of temperature and seawater $\delta^{18}O$ on *Donax obesulus* (Reeve, 1854) shell $\delta^{18}O$

Jacob P. Warner^{a,*}, Kristine L. DeLong^{a,d}, David Chicoine^a, Kaustubh Thirumalai^b, C. Fred T. Andrus^c

- ^a Department of Geography and Anthropology, Louisiana State University, Baton Rouge, LA, USA
- ^b Department of Geosciences, University of Arizona, Tucson, AZ, USA
- ^c Department of Geological Sciences, University of Alabama, Tuscaloosa, AL, USA
- ^d Coastal Studies Institute, Louisiana State University, Baton Rouge, LA, USA

ARTICLEINFO

Editor: Michael E. Boettcher

Keywords: Oxygen Isotopes Bivalve Mollusk Sclerochronology ENSO Peru

ABSTRACT

The coastline of Peru lacks long-lived marine organisms useful for paleoclimatic reconstructions generating a need for novel archives. Short-lived (<5 years) bivalves are commonly found in geological and archaeological deposits and thus can provide "snapshots" of past climatic variability (i.e., seasonal range), similar to data obtained by individual foraminifera analysis, rather than continuous, cross-dated time series (e.g., trees and corals). Previous studies have found success using the short-lived intertidal clam Mesodesma donacium. However, M. donacium are vulnerable to die-offs from the warmer sea surface temperatures (SST) associated with El Niño events and are functionally extinct in northern Peru thus limiting the possibility of modern analog studies for that region. Here we investigate the short-lived (1-3 years) surf clam, Donax obesulus, commonly found in northern Peru, as a paleoclimate archive. Donax obesulus populations are able to survive the warmer SSTs present during El Niño years although they are vulnerable to colder SSTs associated with La Niñas. We assessed the environmental drivers underlying subannual δ^{18} O variability in *D. obesulus* from live collected shells from fish markets and coastal beaches near the Nepeña Valley, Peru in 2012 (La Niña), 2014 (ENSO-neutral), and 2016 (El Niño). Forward modeling of pseudo-shell δ^{18} O reveals that SST variations are a dominant driver with secondary contributions from seasonally-varying seawater $\delta^{18}O$ ($\delta^{18}O_{sw}$). By accounting for varying $\delta^{18}O_{sw}$, we isolated the temperature dependent variable resulting in a paleotemperature equation for D. obesulus δ^{18} O. We verified our results with the δ^{18} O record of a *D. obesulus* shell collected in 2006. Our results suggest that the paleotemperature equation we developed is useful for reconstructing El Niño-Southern Oscillation (ENSO)-related climatic variations in this region and the pseudo-shell approach may be useful for understanding shell δ^{18} O in other locations.

1. Introduction

Sclerochronology (the study of accretionary hard parts) has emerged as a useful tool for developing paleoclimate reconstructions, similar to dendrochronology (the study of tree-rings), to establish a biological chronology for that organism (Buddemeier et al., 1974; Hudson et al., 1976; Jones, 1983). The physical and chemical variations along that biological chronology may record the environmental conditions, such as temperature, when that layer was formed and thus has come to be known as sclerochemistry (Gröcke and Gillikin, 2008). Bivalve shells typically form layers as they grow and thus contain a record of the environment. These geochemical proxies can be assigned a date of

occurrence thus forming a paleoclimate reconstruction (Schöne, 2008; Schöne and Gillikin, 2013; Schöne and Surge, 2014). Long-lived bivalves have been used to build reconstructions of temperature, pollution, climate patterns, upwelling and other parameters (e.g., Butler et al., 2013; Reynolds et al., 2013; Schöne et al., 2011; Steinhardt et al., 2016). Although they have provided valuable environmental information on interannual to centennial time scales (Schöne et al., 2003), bivalve shells can also be used to reconstruct information on seasonal cycles and intraannual climate variability (Butler and Schöne, 2017).

Short-lived (<5 years) bivalves have emerged as a novel and robust paleoceanographic and climatological archive available for coastal Peru (e.g., Carré et al., 2012b, 2013; Carré et al., 2014; Etayo-Cadavid et al.,

E-mail address: jwarn11@lsu.edu (J.P. Warner).

^{*} Corresponding author.

2013; Etayo-Cadavid et al., 2018). Whereas their relatively short lifespans make long temporal reconstructions difficult (though, not impossible see Schöne, 2003), their ability to record environmental signals over the course of a year or more makes them useful to reconstruct seasonal to interannual environmental variability (Carré et al., 2012a; Carré et al., 2013). Stable oxygen isotope values (δ^{18} O) in shells of most bivalve species vary on intra- and interannual time scales in equilibrium with sea surface temperature (SST) after accounting for the δ^{18} O value of ambient seawater (δ^{18} O_{sw}) during shell biomineralization (Epstein et al., 1953; Grossman and Ku, 1986; Mook and Vogel, 1968; White et al., 1999). Seawater δ^{18} O values can vary with evaporationprecipitation, ocean advection, upwelling, and fluvial input in coastal areas, all of which are influenced by El Niño-Southern Oscillation (ENSO) variability in coastal Peru. The ubiquitous presence of shortlived bivalves and other mollusk shells in Peruvian archaeological sites spanning the Holocene Epoch makes them uniquely positioned to leverage the reconstruction of past climatic shifts and variability coeval with human-environment dynamics (Carré et al., 2009; Sandweiss, 2003; Sandweiss and Kelley, 2012; Sandwess et al., 2001).

Previous researchers in Peru targeted the surf clam Mesodesma donacium (known locally as machas), an intertidal bivalve that can live for up to five years. Unfortunately, due to fisheries pressure and increased El Niño frequency and intensity since the 1980s M. donacium are functionally extinct (Riascos et al., 2008, 2011; Tarifeño-Silva, 1980) north of ~16°S (Fig. 1), thereby limiting the opportunity for modern analog studies. However, there are other extant short-lived mollusks frequently recovered from archaeological contexts in northern Peru (Chicoine and Rojas, 2012, 2013; Roselló et al., 2001). In this paper, we examine the $\delta^{18}\text{O}$ signals recovered from individuals of one such bivalve species, Donax obesulus, and discuss how these variations are driven by environmental signals including SST, $\delta^{18}O_{sw}$, and oceanographic processes related to ENSO phase. Understanding these factors is crucial for refining the utility of Donax obesulus as a potential paleoclimatic archive, especially given the complexities of the oceanography along the Peruvian coastline.

The goals of this study are thus:

J.P. Warner et al.

- 1) To assess the relationship between *D. obesulus* $\delta^{18}O$ and SST and within the range of $\delta^{18}O_{sw}$ variations in the region and assess the influence of $\delta^{18}O_{sw}$ on shell $\delta^{18}O$.
- 2) To develop a paleotemperature equation for *D. obesulus* and identify uncertainties in its use for paleoclimate reconstruction.

1.1. Eco-climatology and biology of Donax obesulus

Our study area is located in coastal Ancash, a region of northern Peru. Local SST (1952-1987, 1996-2018; 1 m water depth; 9.08°S, 78.61°W, 250 m offshore, 20 km north of the study region; IMARPE, 2019; Domínguez et al., 2017) and satellite sea surface salinity (1° x 1° SSS; Zuo et al., 2019) records show that oceanographic and climatic conditions are fairly uniform for the coastal region during non-ENSO years (68.6% of all months) with monthly SST ranging from 18 to 22 °C (Fig. 2B). During strong El Niño events, SST can exceed 25 °C for several months (3.1% of all months) whereas during strong La Niña events SST can drop below 16 °C, though only rarely (1% of all months). Salinity ranges from 34 to 35 psu (Fig. 2A), though occasional extreme precipitation events can drive salinity down to 33 psu (Grados et al., 2018). In this region, La Niña events can cause drought conditions lasting for months that increase salinity up to 35 psu, and on the other hand El Niño events increase precipitation and river runoff into the coastal environment that causes a decrease in salinity down to 34 psu. ENSO usually produces compounded cold-dry (i.e., more saline) and warm-wet (i.e., less saline) conditions driven by La Niña and El Niño events, respectively in this region (Fig. 2). These changes from cold-dry to warm-wet conditions produce an additive signal in the δ^{18} O of carbonate shells of marine mollusks such that as temperature increases and salinity decreases the shell $\delta^{18}O$ ($\delta^{18}O_{shell}$) values become relatively lower and vice versa. Occasionally, highland pluvial events can cause freshening signals in coastal areas (March to May 2012, Fig. 2) during La Niña years; however, these anomalies are present in the SSS data as decreases in salinity. Additionally, there is evidence that central Pacific La Niña events can drive precipitation increases in coastal Peru similar

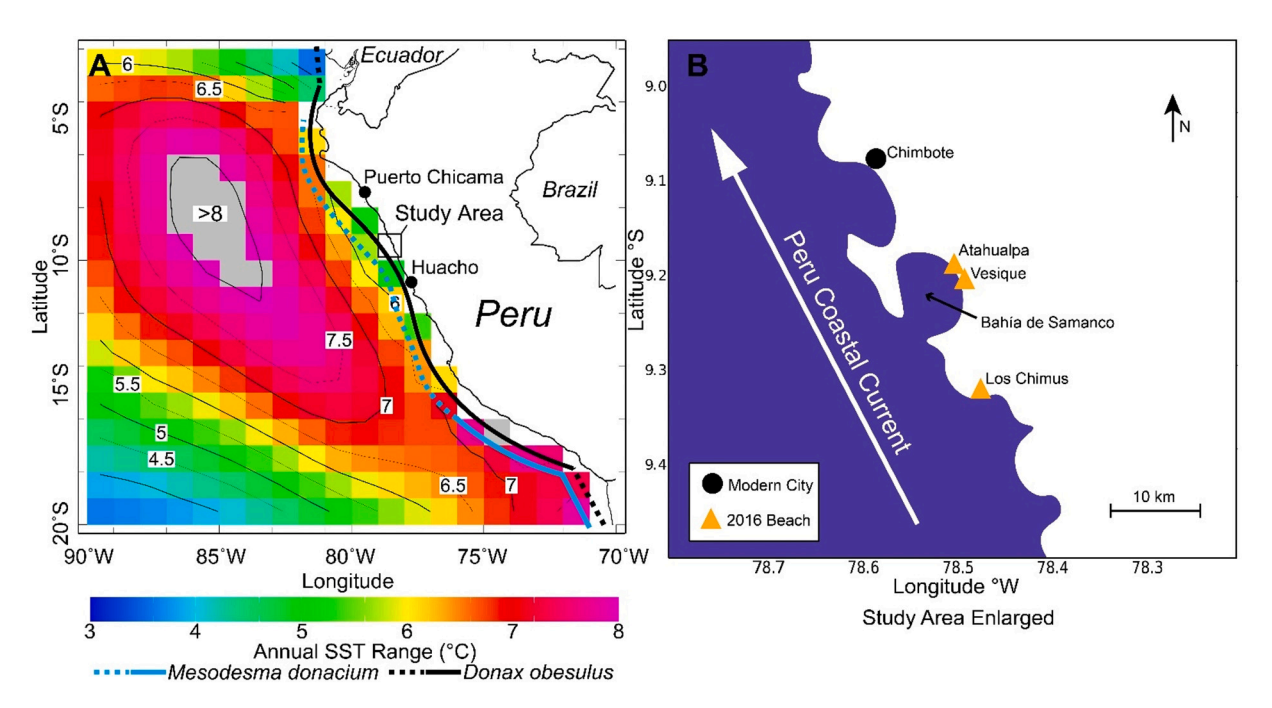


Fig. 1. (A) Biological ranges of the bivalve species examined and (B) our study area in northern coastal Peru. (A) The average annual (or seasonal) range of SST from the World Ocean Atlas 2009 (Locarnini et al., 2010) climatology are plotted as the annual range of SST is a target metric for short-lived bivalve reconstructions. The historical (dashed) and current (solid) ranges of *M. donacium* (cyan) and *Donax obesulus* (black) (Carstensen et al., 2010) are shown along the coast. (B) Shells were purchased in Chimbote in 2012 and 2014, and IMARPE maintains a monitoring station for SST nearby. The beaches where live shell collection occurred in 2016 are marked with orange triangles. (For interpretation of the references to colour in this figure legend, the reader is referred to the web version of this article.)

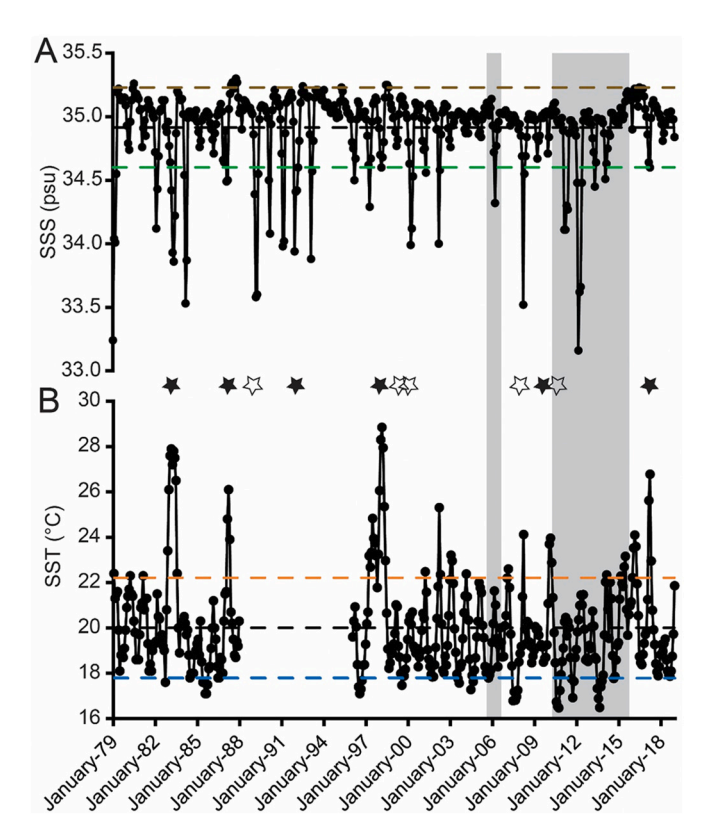


Fig. 2. (A) Monthly SSS from the European Centre for Medium-Range Weather Forecasts (ECMWF) Ocean Reanalysis System 5 (ORAS5) (Zuo et al., 2019) for the 1° grid cell centered on 9.5°S, 79°W and (B) monthly SST from the Instituto del Mar del Peru (IMARPE) decentralized laboratory in Chimbote, Peru (IMARPE, 2019), see Fig. 2 for location. In (A) and (B), black dashed lines represent the mean of each record, whereas the colored dashed lines represent 1 standard deviation of each record. The gray shaded areas are this study's time interval and the verification time interval. Black stars represent strong El Niño ($\geq + 1.5~^\circ \text{C}$) events and unfilled stars represent strong La Niña ($\geq -1.5~^\circ \text{C}$) events.

to eastern Pacific El Niño events (Lavado-Casimiro and Espinoza, 2014).

Donax obesulus is a short-lived, aragonitic, intertidal bivalve that occupies the surf zone of dynamic, sandy beaches from southern Ecuador to southern Peru (Fig. 1A), and on occasion into northern Chile (Coan, 1983; Etayo-Cadavid et al., 2013; Talledo, 1980). Donax obesulus is an important species for present-day artisanal fisheries and foodways. Despite their relatively small size (~15 mm × 30 mm), these clams have been consumed by populations along the Peruvian coast for millennia (Sandweiss et al., 2001). Previous research (Coan, 1983; Paredes and Cardoso, 2001) suggests the existence of at least two separate species (D. obesulus and D. marincovichi, sometimes also D. peruvianus); although, a recent study (Carstensen et al., 2009) posits that these are separate ecomorphs of the same species. We follow the recommendation of Carstensen (2010) in using the designation D. obesulus.

Whereas internal increments are usually used as a marker for seasonal growth in bivalves (Schöne, 2008), *D. obesulus* growth increments are difficult to interpret and thus not necessarily useful for time assignment outside of general age at capture (i.e., if there is an annual growth increment in the shell it is likely at least one year old). Other methods for estimating age and growth rates are thus necessary when discussing *D. obesulus* growth and age estimation. Previous research has identified von Bertalanffy (1957) growth curves as a useful tool for understanding bivalve growth patterns in other species (Palmer et al., 2021). Various length-age studies using von Bertalanffy growth curves for *D. obesulus* (Arntz et al., 1987; Paz and Alzamora, 2014; Paz et al., 2007; Ramírez et al., 2016) set the theoretical upper age limit at

approximately 36 months, with most individuals living less than 24 months. The study of Paz and Alzamora (2014) generated a von Bertalanffy growth curve for *D. obesulus* based on specimens they collected between 2001 and 2009 in the Bahía de Samanco, which is located in our study area (Fig. 1B). Their growth curve is based on a repeated length-age assignment of size classes (in 1 mm intervals) sampled annually and they calculated *D. obesulus* shells reach a length of 22 mm at one year of age. They included shells from an 8-year study window that included La Niña, ENSO-neutral, and El Niño conditions (NOAA, 2020) thus averaging out any potential bias related to ENSO phases that could influence their *D. obesulus* growth curve and equation.

1.2. Previous D. obesulus and Donax spp. geochemical studies

Some studies have examined $\delta^{18} O_{\text{shell}}$ and other geochemical signals in D. obesulus and other species of the genus Donax. Perrier et al. (1994) examined whole shell $\delta^{\hat{1}8}$ O for *D. obesulus* among other species from both modern and archaeological samples as a proxy for SST and found a correlation with modern local mean annual SST when using the Epstein et al. (1953) equation for calcium carbonates. Other geochemical studies using D. obesulus investigated pre-bomb radiocarbon signals as an upwelling proxy along with internal shell δ^{18} O profiles as SST range indicators using the Grossman and Ku (1986) and Böhm et al. (2000) equations for mollusks (Etayo-Cadavid et al., 2013; Etayo-Cadavid et al., 2018). Those authors note that there is no correlation between the two proxies suggesting that fast water mixing on a time scale of 40-90 days equilibrates water temperature before radiocarbon from the atmosphere can equilibrate with seawater (Etayo-Cadavid et al., 2018). Furthermore, other studies suggest species-specific δ^{18} O-SST equations are needed for accurate paleotemperature reconstruction in mollusks (Carré et al., 2005a, 2005b; Chamberlayne et al., 2021; Royer et al., 2013; Tynan et al., 2014).

Efforts to develop geochemical proxies for temperature in other Donax spp. have produced equivocal results. Jones et al. (2005) found strong correlations between SST and the $\delta^{18}O_{shell}$ of modern *Donax* variabilis from northeast Florida using the mollusk-specific paleotemperature equation developed by Grossman and Ku (1986). On the other hand, Galimberti (2010) found the $\delta^{18}O_{shell}$ profiles of *Donax serra* from South Africa required an offset of 0.7% when using the Grossman and Ku (1986) equation to correlate to SST that they attribute to vital effects. Jew et al. (2016) tested the $\delta^{18}O_{shell}$ -SST relationship of *Donax* denticulatus from the Caribbean Island of Nevis using various published temperature equations and found SST reconstructed from δ¹⁸O_{shell} was statistically indistinguishable from SST recorded at their study site when using Eq. 1 of Grossman and Ku (1986). Combined, these studies highlight the potential of the genus Donax but also the necessity of a closer examination of the $\delta^{18}O_{shell}$ relationship to temperature and $\delta^{18}O$ of seawater ($\delta^{18}O_{sw}$). Whereas D. obesulus is expected to precipitate their shells in equilibrium with seawater like other aragonitic mollusks (Mook and Vogel, 1968), these studies also illustrate that species-specific vital effects alongside variability in local $\delta^{18}O_{sw}$ are important factors to consider.

Each of these aforementioned *Donax* studies employed different sampling strategies, a tenet that may partly explain the diversity of their $\delta^{18}\text{O-SST}$ calibration results, as has been found with other marine carbonates and mollusks (Twaddle et al., 2016). Jones et al. (2005), Jew et al. (2016), and Etayo-Cadavid et al. (2013, 2018) micromilled the convex outer surface of the shell without taking cross-sections to extract samples for $\delta^{18}\text{O}$ analysis. Galimberti (2010) cut *D. serra* shells into thin cross-sections and then hand-milled them (i.e., Dremel TM tool) along the growth increments to remove samples. In our study, given the success of similar micromilling methods in larger bivalve species (Carré et al., 2005a, 2005b; Hallmann et al., 2009; Schöne et al., 2005), we use thick cross-sections of *D. obesulus* micromilled at approximately monthly intervals to extract enough shell material for $\delta^{18}\text{O}$ analysis.

In this study, we first generate growth models for each shell using the

previously determined von Bertalanffy growth equation for *D. obesulus* (Paz and Alzamora, 2014) to confirm that the shell's $\delta^{18}O$ values span at least 12 months and to assign time to each shell chronology. To better understand the environmental signal driving the $\delta^{18}O_{\text{shell}}$ values, we construct a forward model (pseudo-shell) based on observed SST and SSS-calculated $\delta^{18}O_{\text{sw}}$, similar to methods that are used in shell, coral, and foraminifer studies (e.g., Carré et al., 2012a; Peharda et al., 2019; Thirumalai et al., 2013; Thompson et al., 2011) to calculate expected $\delta^{18}O_{\text{shell}}$ values. Finally, we assess and validate the paleotemperature calibration equations based on the application of observed seasonal $\delta^{18}O_{\text{sw}}$ values from the region.

2. Materials and methods

2.1. Specimen collection

D. obesulus are relatively easy to capture, only requiring an individual to wade up to about one meter of seawater depth and dig about 50 mm into the sandy substrate. Specimens of D. obesulus were collected live from beaches (July 2016) or purchased alive (August 2012 and July 2014) from the La Sirena fish market in Chimbote, Department of Ancash, Peru. Live collections come from two beaches (Vesique and Atahualpa) along the Bahía de Samanco of the Nepeña Valley, Department of Ancash, Peru and one slightly farther south (Los Chimús). Those purchased at the fish market come from the Bahía de Samanco, making specimens from all three years geographically comparable (Fig. 2B). Each collection of shells (2012, 2014, and 2016) were purchased or collected during one day thus we assume the same death day for each collection.

2.2. Specimen preparation and sampling

After collection or purchase, we sacrificed specimens, removed their meat, dried the shells, and then packed them into Whirlpaks TM (sterile collection bags) for transport. In the lab, we rinsed the shells with deionized water, manually removed any remaining visible flesh, and cleaned them with a Branson 400 sonifier digital ultrasonic cell disruptor in deionized water to remove any remaining tissue. This cleaning method does not introduce possible isotopic shifts that can occur with oxidative cleaning or other chemical cleaning methods (Roberts et al., 2018). We then dried the shells in an oven at 40 $^{\circ}$ C for 12 h. Left valves from six specimens from each collection year (total = 18) were selected for further analysis based on their larger shell size and integrity (no signs of predation, parasitism, or damage). Selected valves were set into West System TM two-part epoxy for 12 h. Next, we cut two thick sections from each shell, each ~1 mm thick, along the axis of maximum height from the umbo to the ventral margin of the left valve of each specimen (Fig. 3A) using a Buehler Isomet slow speed saw equipped with a diamond-edged blade. One thick section was processed for imaging growth increments and archival purposes and the other thick section for microsampling for isotopic analysis. Both sections were cleaned in a sonicator bath without heat to remove cuttings.

Individual *D. obesulus* shells often do not generate readily visible increments due to their short lifespan and ecological niche in swash and surf zones, yet tidal increments and annual growth checks can be present. The visibility of these increments is minimal without processing of thick sections using methods that render them unsuitable for geochemical analysis via micromill sampling (e.g., making them too thin, or possible alteration of primary chemistry via cleaning and

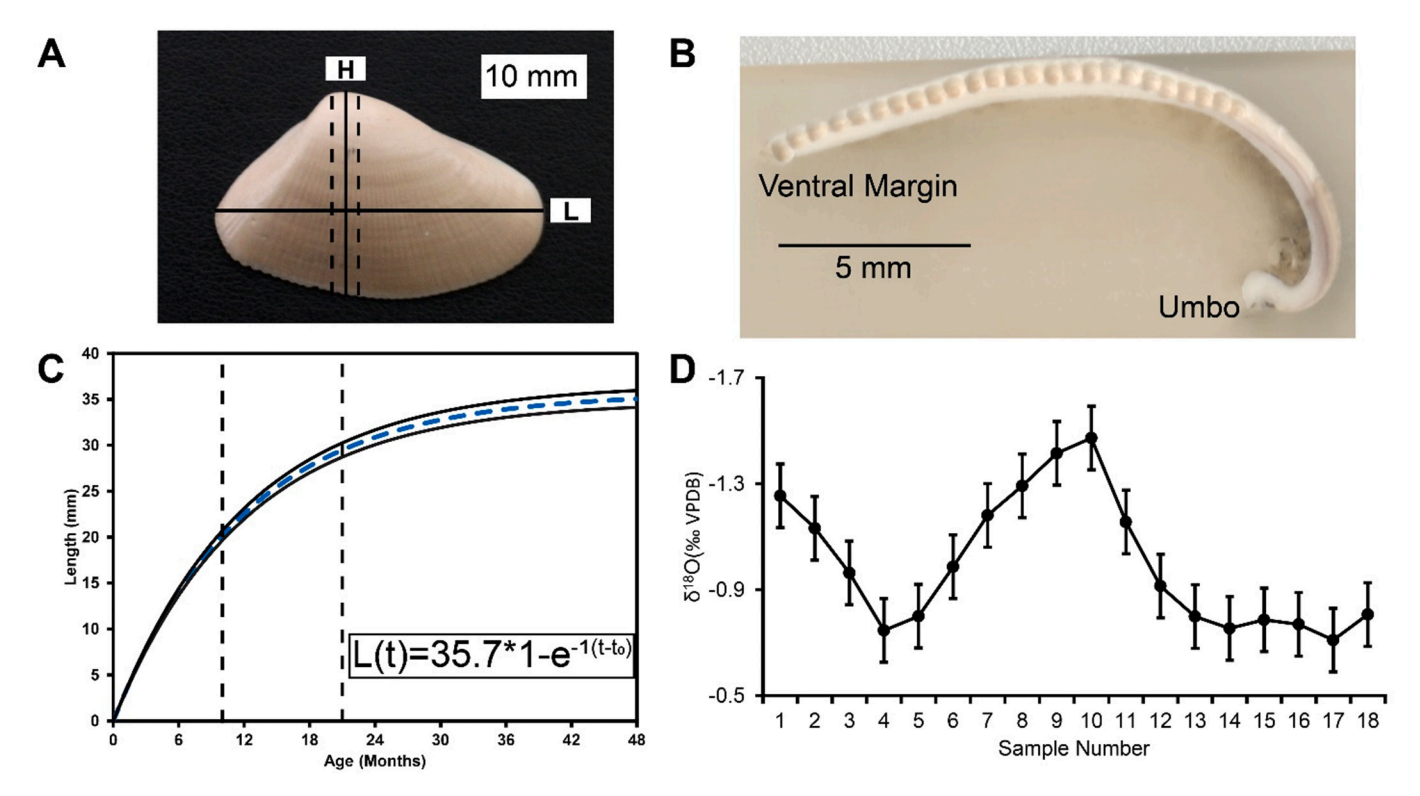


Fig. 3. An example of our sampling method. (A) Dashed lines represent cuts taken for cross-sections, L is the length for von Bertalanffy growth calculation, H is the axis of maximum height for H/L ratio. (B) Shell after cross-sectioning and micromill sampling (drill bit size 0.5 mm) for isotopic analysis. (C) The blue dashed line is the von Bertalanffy growth curve for *Donax obesulus* (Paz and Alzamora, 2014) used for $\delta^{18}O_{shell}$ time assignment. Black dashed lines represent the youngest (\sim 10 months) and oldest (\sim 21 months) shells determined in this study. The error envelope (black solid lines) is a 2.6% relative standard deviation (RSD) based on population shell H/L ratio measurements. Length is measured in mm as in (A) and is a function of age (t) in months. (D) An example of the raw $\delta^{18}O$ determinations for one shell from the shell edge (1 = most recently grown shell) towards the umbo (18 = earliest shell growth), error bars are analytical precision (0.12‰, 2 σ). The $\delta^{18}O$ axis is reversed so that warmer values are up. (For interpretation of the references to colour in this figure legend, the reader is referred to the web version of this article.)

polishing if temperatures exceed 100 °C (Waite and Swart, 2015)) or staining. We thus used a second thick section for imaging. As a result, we only used increments that were visible when specimens were manually polished with silicon carbide powder (14, 10, 8.0, and 1.0 μ m) for time assignment and life span assessment. Specifically, we used annual growth checks as an indicator of at least one year of growth.

We sampled each shell using a 0.5 mm carbide drill bit mounted on a TAIG Micromill $^{\text{TM}}$ guided by SuperTech SuperCam XP software (DeLong et al., 2011). Sample paths were drawn in the micromill software as either points or lines at 0.5 to 1.0 mm intervals and then computer milled to a depth of 0.5 to 1.0 mm (Fig. 3B). The resulting shell cuttings (\sim 80 µg for analysis and an archive aliquot) were collected using a scoopula and placed into microcentrifuge tubes for storage. Sampling paths were drawn (length and sampling depth) to span as much of the shell's cross-section as possible guided by growth checks (areas of tight bundles of increments) and increment patterns when visible.

2.3. Time assignment

To assign time to our samples, we used the von Bertalanffy (1957) growth equation calculated for *D. obesulus* by Paz and Alzamora (2014). This equation was developed using the length at capture of individuals collected live in Samanco Bay from 2001 to 2009 and includes the three phases of ENSO (Paz and Alzamora, 2014). To adjust the growth equation to our sampling strategy, we applied the height to length ratio of each shell sampled in this study to the expected length at daily resolution. We then calculated how many days a 0.5 mm sampling interval would span from the calculated age at capture (i.e., oldest shell age sample) to the most interior sample (i.e., youngest shell age sample) along the axis of maximum height.

2.4. Stable isotope analysis

Shell samples were dissolved in phosphoric acid at 70 °C and analyzed at the Stable Isotope Geosciences Facility at Texas A&M University on a Thermo Scientific MAT 253 equipped with a Kiel IV device. Data were adjusted using an empirical slope measured vs the known Vienna PeeDee Belemnite (VPDB) standard. Analytical precisions are $\pm 0.06\%$ (1 σ) for $\delta^{18}O$ and $\pm 0.04\%$ (1 σ) for $\delta^{13}C$ based on long-term, replicate (6 samples/day) analyses of carbonate standards NBS-19 ($\delta^{18}O=-2.20\%$, $\delta^{13}C=1.95\%$) and IAEA-603 ($\delta^{18}O=-2.37\pm0.04\%$, $\delta^{13}C=2.46\pm0.01\%$). All isotopic values are reported in delta notation as per mil units (‰) relative to the VPDB isotopic standard.

3. Results

3.1. Sample temporal resolution

Growth modeling using shell growth checks and the growth equation of Paz and Alzamora (2014) provided an estimate of the number of days per sample and showed our sampling method yielded at least one annual cycle in $\delta^{18}\text{O}$ per shell. We obtained isotopic measurements ($\delta^{18}\text{O}$ and $\delta^{13}\text{C}$) for 18 shells (six each for 2012, 2014, and 2016) with the number of samples per shell varying from 12 to 26 (Tables S1–S3), a sampling resolution of 22 samples per year on average. The growth models suggest that we were able to sample between 175 and 460 days from each shell, with an average of 350 days per shell. Each sample represented 17 days on average (±6 days, 1 σ ; range from 9 to 42 days) (Tables S1-S3).

3.2. Stable isotope results

Correlations between raw $\delta^{18}O_{shell}$ and $\delta^{13}C_{shell}$ for each shell varied from 0.79 to -0.81 among all 18 shells suggesting the lack of a consistent relationship (Tables S1-S3). Interpretation of $\delta^{13}C_{shell}$ is not straightforward and will not be examined further in this report; however, the data are included in the supplementary information for

posterity (Tables S1–S3).The raw shell δ^{18} O values (Table 2; Fig. 4) show subtle seasonal differences for each of the three intervals investigated. In 2012 (La Niña), between 18 and 26 samples per shell were analyzed with an average δ^{18} O_{shell} of -1.01% ($\pm 0.35\%$, 1σ) and average range of 0.98% ($\pm 0.24\%$, 1σ). In 2014 (Neutral), between 18 and 23 samples per shell were analyzed with an average δ^{18} O_{shell} of -1.09% ($\pm 0.31\%$, 1σ)

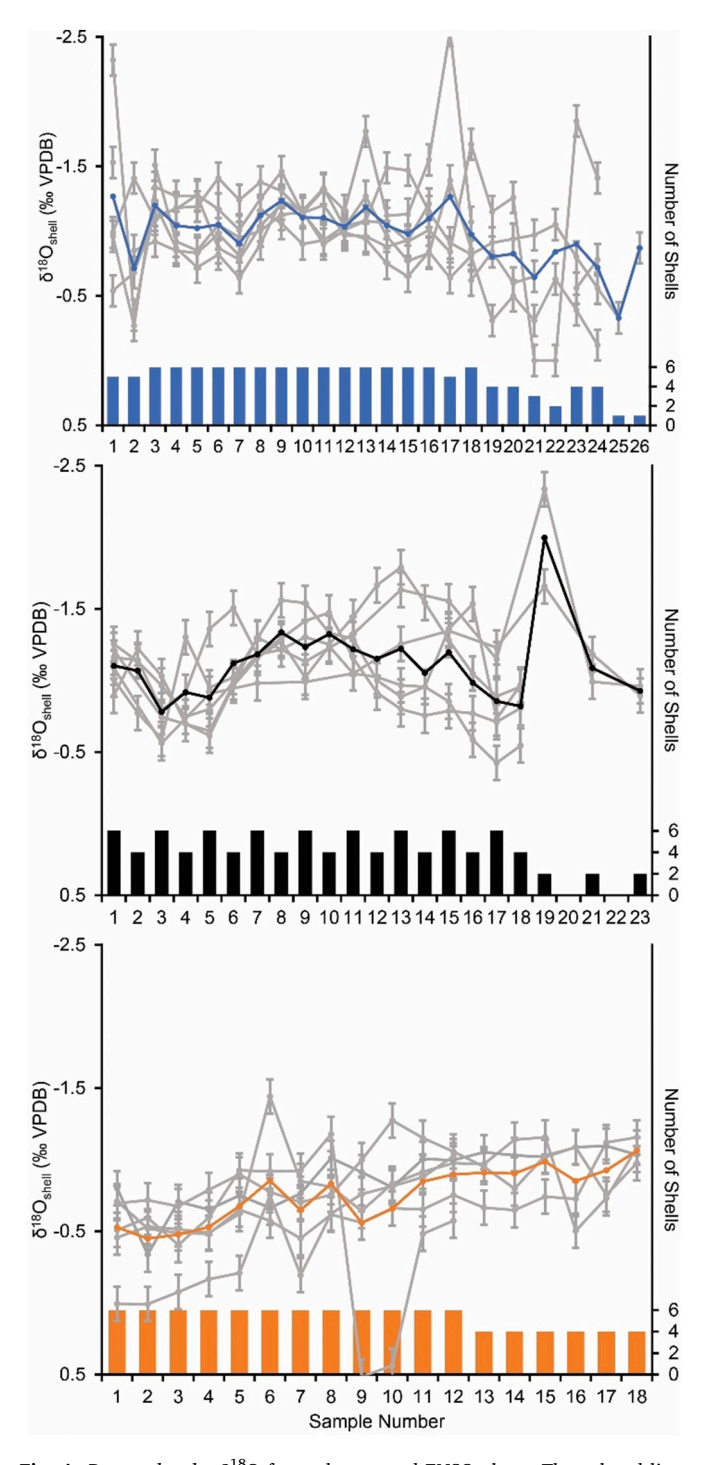
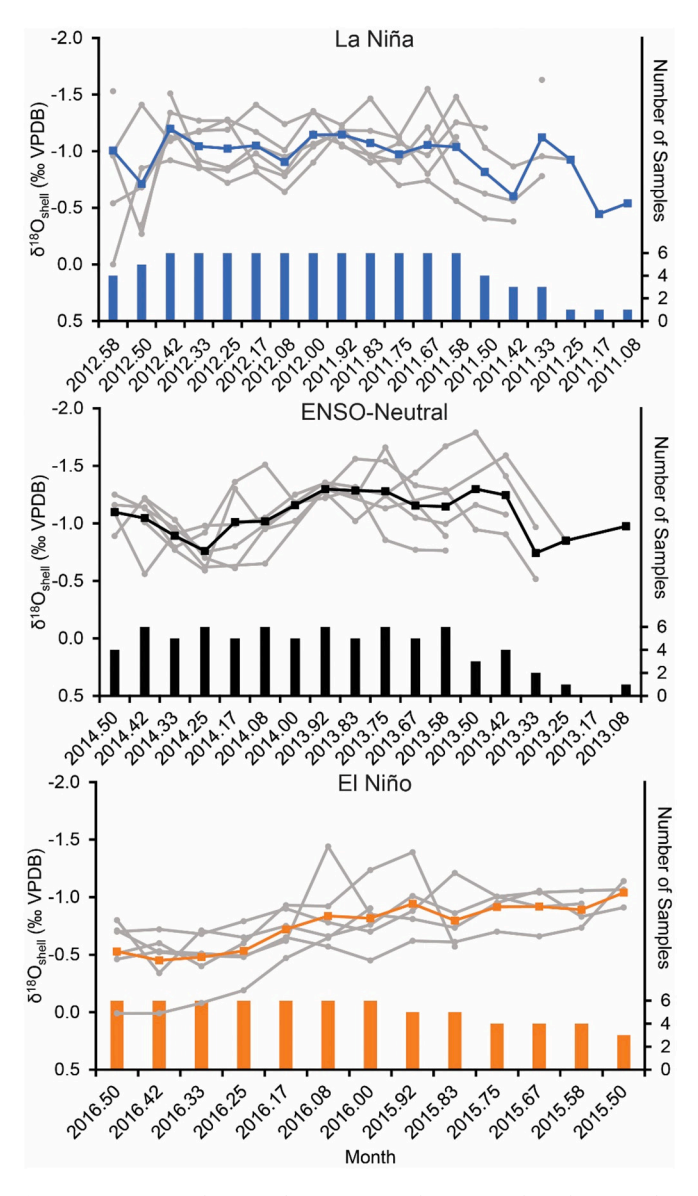


Fig. 4. Donax obesulus δ^{18} O for each year and ENSO phase. The colored lines are the average for each year and the light gray lines represent individual shell δ^{18} O records. Top: 2012, Middle: 2014, and Bottom: 2016 collected shells. Sample 1 is from shell edge and the most recent sample. The collection date and sample numbers increase towards the umbo (i.e., shell growth is youngest to oldest from right to left). The δ^{18} O axes are reversed so that warmer values are up. The secondary y-axis is the number of samples used to calculate the mean for that sample number. Error bars are analytical precision (0.12‰, 2 σ).

and average range of 0.90‰ ($\pm 0.21\%$, 1σ). In 2016 (El Niño), between 12 and 18 samples per shell were analyzed with an average $\delta^{18}O_{shell}$ of -0.70% ($\pm 0.33\%$, 1σ) and average range of 0.80‰ ($\pm 0.31\%$, 1σ). In general, the $\delta^{18}O_{shell}$ for each interval has similar annual cycles with increasing disagreement among contemporaneous samples as the sample number from the ventral edge increased (assumed to be the same day), especially after the 12th sample. For each set of contemporaneous samples, the differences in shell $\delta^{18}O$ are less than analytical precision (2σ), especially for the first ~ 12 samples that should be approximately the same time interval. In 2016 (El Niño), the seasonal cycle is relatively flat with an overall more positive mean $\delta^{18}O_{shell}$. In 2012 (La Niña) and 2014 (Neutral), the seasonal cycle contains subtle but visible winter and summer shifts.

3.3. Sample time assignment

To achieve approximately monthly δ^{18} O values for comparison to monthly SST records (Fig. 5), samples representing less than 60% (17 days) of one month (28 days) were averaged together (n=196) with the next sample of a similar time span. We physically resampled any sections representing more than 150% (42 days) of one month (n=2) at a higher



 $\begin{tabular}{ll} Fig. 5. As in Fig. 4 but samples are assigned to a month and averaged to monthly values as needed. \\ \end{tabular}$

resolution (i.e., with a smaller spatial increment of sample sizes) on the reverse side of the thick section. We included those samples rather than the original lower resolution samples in our analysis. If physical resampling was not possible, we omitted those samples from the analysis (n=1).

4. Discussion

4.1. $\delta^{18}O_{shell}$, SST, and $\delta^{18}O_{sw}$

The seasonal cycle among contemporaneous shells is similar suggesting a common environmental forcing that is distinct for each time interval (Fig. 4). We first assess the influence of SST alone on the growthmodeled Donax obesulus $\delta^{18}O_{shell}$ via calculation of Pearson's correlation coefficient between monthly SST and monthly average $\delta^{18}O_{shell}$. Most (83.3%) of our individual monthly growth-modeled $\delta^{18}O_{\text{shell}}$ records do not correlate with local SST (IMARPE, 2019) at the 5% significance level (77.8% do not correlate at the 10% significance level) (Table 1) nor does the averaged $\delta^{18}O_{shell}$ for each year. This lack of correlation may be partly due to uncertainty in the growth model used to assign time to each shell δ^{18} O value (Fig. 3) or the fact we did not align the shell δ^{18} O to SST for time assignment as is done with other proxies (e.g., corals, and coralline algae) or the low number of samples increasing the threshold for a correlation to be significant. In the 2012 and 2014 shells, SST and $\delta^{18} O_{shell}$ diverge approximately 7 to 10 months before sample collection, or during the austral winter (Fig. 6). However, in the 2016-collected shells, the preceding austral summer (3-9 months prior to collection) is the point where divergence occurs (Fig. 6). This seasonal divergence suggests a seasonal influence of $\delta^{18}O_{sw}$ on $\delta^{18}O_{shell}$.

To understand the environmental forcing driving our *Donax obesulus* $\delta^{18}O$ values, we generated "pseudo-shell" forward models (akin to pseudo-corals as in Thompson et al., 2011 or calculated $\delta^{18}O$ as in Goodwin et al., 2003 and Peharda et al., 2019) of the expected $\delta^{18}O$ for each of the time intervals (2011–2012, 2013–2014, and 2015–2016) during which the shells grew. For temperature, we used monthly SST from Chimbote (IMARPE, 2019), close to our study site (Fig. 2). We first developed these forward models using the $\delta^{18}O$ -SST equation (Eq. 1) developed by Grossman and Ku (1986), then also used that developed by Carré et al. (2005a, 2005b) for *M. donacium* (Eq. 2), as it is the only such equation developed for an intertidal bivalve species in western South

Table 1 Pearson's correlations for monthly growth-modeled $\delta^{18}O_{\rm shell}$ and monthly average SST.

Shell	Correlation	P	n
VBTB12-17	-0.02	0.95	15
VBTB12-25	-0.15	0.63	13
VBTB12-37	0.24	0.41	14
VBTB12-118	0.12	0.70	13
VBT12-270	0.13	0.61	18
VBTB12-360	-0.59	0.02	15
CMD14-8	-0.53	0.08	12
CMD14-123	0.28	0.47	9
CMD14-129	0.05	0.87	14
CMD14-134	0.51	0.05	15
CMD14-142	-0.17	0.57	14
CMD14-144	0.17	0.61	12
16AP-6	-0.48	0.10	14
16AP-26	0.25	0.42	14
16AP-37	0.01	0.98	14
16AP-51	-0.05	0.88	12
16AP-71	-0.66	0.06	9
16LC-168	-0.88	0.01	7
Interval averages	0.99	0.09	3

Note: Shells highlighted in light gray are significant at the 5% level and in dark gray are significant at the 10% level. SST from Chimbote, Peru (IMARPE, 2019).

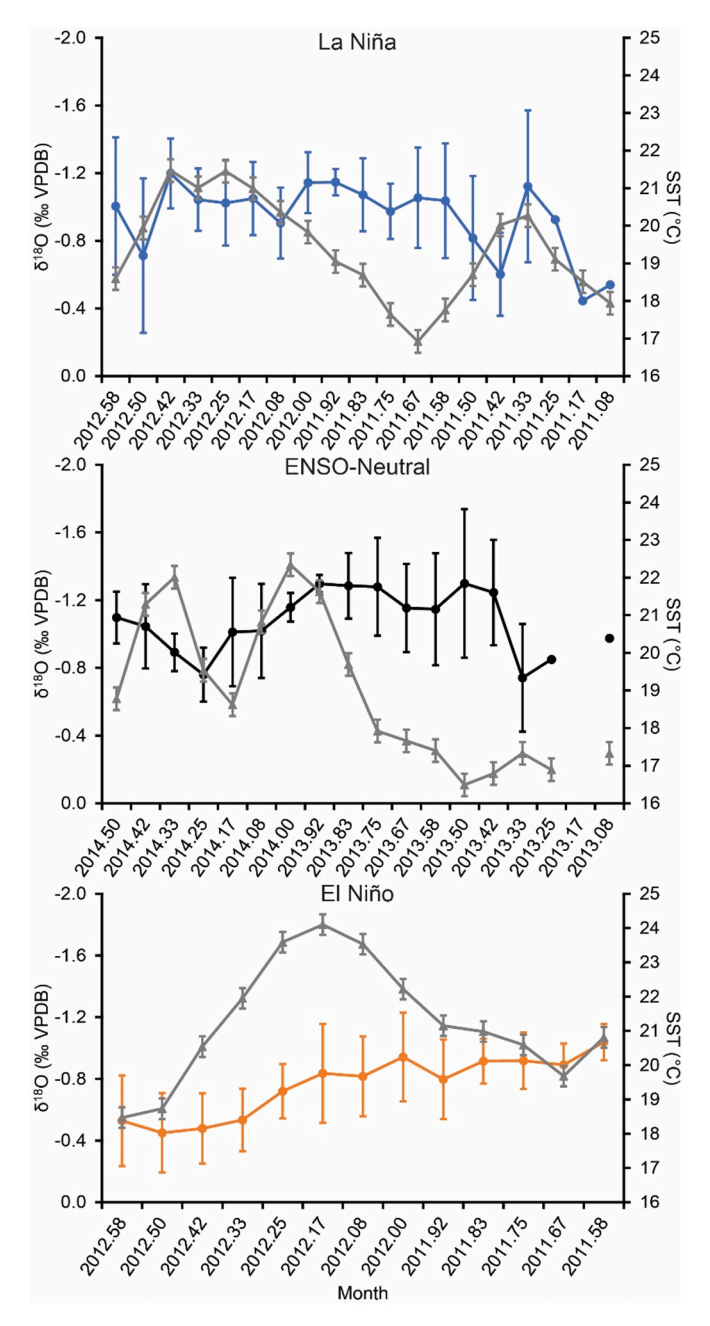


Fig. 6. Comparison of average monthly $\delta^{18}O_{\text{shell}}$ (color circles) with monthly average SST (gray triangles). Error bars for $\delta^{18}O_{\text{shell}}$ are one standard deviation of the mean for each month (for n>2, otherwise not given), whereas error bars for SST are $\pm 0.3\,^{\circ}\text{C}$ based on instrumental precision. The monthly SST is from the IMARPE decentralized laboratory at Chimbote (IMARPE, 2019). The $\delta^{18}O$ axes are reversed so that warmer values are up.

America and both *M. donacium* and *D. obesulus* are aragonitic bivalves (Carré et al., 2005a, 2005b; Etayo-Cadavid et al., 2013). We used the LeGrande and Schmidt LeGrande and Schmidt (2011) $\delta^{18}O_{sw}$ -SSS equation for the tropical Pacific (Eq. 5) to calculate monthly $\delta^{18}O_{sw}$ from the ECMWF ORAS5 (Zuo et al., 2019) monthly SSS product. First, we solved Eqs. 1 and 2 for $\delta^{18}O_{shell}$ resulting in Eqs. 3 and 4 and then determined the $\delta^{18}O$ pseudo-shells records for 2012, 2014, and 2016 from observed SST and calculated $\delta^{18}O_{sw}$.

$$SST = 20.60-4.34 \left(\delta^{18}O_{shell} - \left(\delta^{18}O_{sw} - 0.27\right)\right)$$
 (1)

$$SST = 17.41 - 3.66 \left(\delta^{18} O_{\text{shell}} - \delta^{18} O_{\text{sw}} \right)$$
 (2)

$$\delta^{18}O_{shell} = -0.23(SST) + 4.75 + \delta^{18}O_{sw} + 0.27$$
(3)

$$\delta^{18}O_{\text{shell}} = -0.27(SST) + 4.76 + \delta^{18}O_{\text{sw}}$$
(4)

$$\delta^{18}O_{sw} = 0.27(SSS) - 8.88 \tag{5}$$

We found that most months of the pseudo shells and observed $\delta^{18}O_{shell}$ did not agree in value, with the Carré et al. (2005a, 2005b) based model outperforming the Grossman and Ku (1986) based model

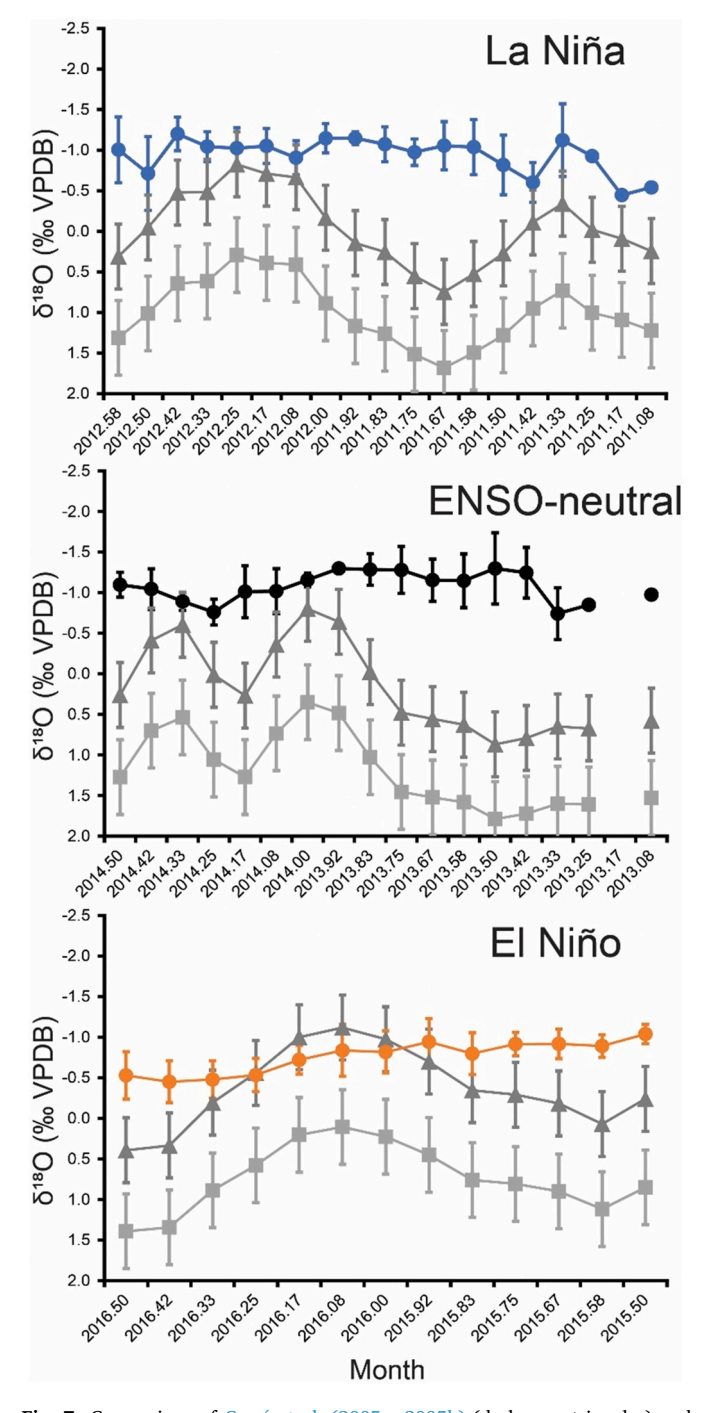


Fig. 7. Comparison of Carré et al. (2005a, 2005b) (dark gray triangles) and Grossman and Ku (1986) (gray squares) modeled $\delta^{18}O_{shell}$ to observed $\delta^{18}O_{shell}$ (colored circles). Organized as in Fig. 6; however, shell model error bars are the root mean square error (RMSE) calculated by Carré et al. (2005a, 2005b) of $\pm 0.40\%$ (1\sigma) and calculated for Grossman and Ku (1986) as $\pm 0.46\%$ (1\sigma). The $\delta^{18}O$ axes are reversed so that warmer values are up.

(Fig. 7) in predicting average $\delta^{18}O_{shell}$. However, the Grossman and Ku (1986) based model did better at predicting the range of $\delta^{18}O_{shell}$, suggesting a difference in slope and intercept would both be necessary to accurately predict *D. obesulus* $\delta^{18}O_{shell}$. We note that after accounting for offsets, the disagreement between predicted and observed $\delta^{18}O_{shell}$ (or residuals) is seasonal, with observed $\delta^{18}O_{shell}$ from the preceding winter more anomalously negative compared to forward-modeled values than warmer seasons.

We next explored the contribution of seasonal changes in $\delta^{18} O_{sw}$ to $\delta^{18}O_{shell}$ with the pseudo-shell model and Eq. 4. We did so because the mean offset between the Carré et al. (2005a, 2005b) based model and our observed values (0.62 \pm 0.26%) is reduced compared to the offset observed with the Grossman and Ku (1986) based model (1.66 \pm 0.24‰) and the $\delta^{18}O_{sw}$ values that would need to be applied to Eq. 1 would be greater than that observed in coastal Peru. To constrain $\delta^{18}O_{sw}$, we held model $\delta^{18}O_{sw}$ to 0‰. The residuals between the SST-only modeled $\delta^{18}O$ values and the observed shell $\delta^{18}O$ values suggest an influence from ambient seasonal δ¹⁸O_{sw} shifts, assuming neither original modeling equation is appropriate for *Donax obesulus*, thus the residuals represent the contribution from $\delta^{18}O_{sw}$ along with error. We then subtracted seasonal δ¹⁸O_{sw} variations for one year (2003) documented by Carré et al. (2013) from Huacho, Peru 240 km south of our research location (Fig. 2) from our observed $\delta^{18}O_{shell}$ values. We do so because this is the only published $\delta^{18}O_{sw}$ data set from Peru that includes seasonal $\delta^{18}O$ values throughout a calendar year. These values vary from 0.03% in the spring to -0.66% in the winter. Unfortunately, there are no additional δ¹⁸O_{sw} data sets from Peru spanning the years of our study, and these data represent an ENSO-neutral year. We thus expanded these values to include those in the range of -0.7 to 0.2% during La Niña and ENSOneutral conditions for our location-based on unpublished $\delta^{18}O_{sw}$ measurements from northern Peru (Fred Andrus-personal communication June 2020).

We used our pseudo-shell models to guide our application of $\delta^{18}O_{sw}$ values, as these models using a negligible $\delta^{18}O_{sw}$ input represented an SST-only approach for the three years of our study (2012, 2014, 2016). For months where there was a residual between the model and observed $\delta^{18}O_{shell}$ values (i.e., pseudo shell – shell = residual), we applied the seasonal $\delta^{18}O_{sw}$ value from the designated range closest to the residual value (e.g., if the difference was -0.8%, we applied a $\delta^{18}O_{sw}$ value of -0.7%). For the 2016 shells, a different approach was needed as the observed values for an ENSO neutral year (-0.7 to 0.2%) did not fit the residuals, thus we applied a set of seasonal $\delta^{18}O_{sw}$ values ranging from

0.0 to 0.6% that represent open ocean conditions in the tropical eastern Pacific (LeGrande and Schmidt, 2006). We do so as we infer the difference between the 2016 model and observed $\delta^{18}O_{shell}$ is driven by advection of open-ocean waters into coastal bays during the 2015–2016 El Niño event (Muis et al., 2018; Peng et al., 2020; Piecuch and Quinn, 2016). As a result of applying these $\delta^{18}O_{sw}$ values, the agreement between $\delta^{18}O_{shell}$ and our forward models was improved (overall $\delta^{18}O_{shell}$ – model r=0.17; after $\delta^{18}O_{sw}$ adjustment r=0.85). These results suggest there are seasonally and interannually varying $\delta^{18}O_{sw}$ shifts and that a single $\delta^{18}O_{sw}$ value cannot be applied to solve for SST (Conroy et al., 2017).

When we subtract $\delta^{18}O_{sw}$ values from $\delta^{18}O_{shell}$ guided by the pseudoshell model residuals (i.e., $\delta^{18}O_{sh\text{-sw}}$) much of the original seasonal and mean variability among individuals and years remains the same for the 2012 and 2014 collected shells. However, there is a statistically significant (using Student's t-test) δ^{18} O shift (-0.33%, t = 3.792, p = 0.001, α = 0.05) in mean values for shells collected in 2016 (Tables 2, S4–S6). For all intervals, the range for $\delta^{18}O_{sh\text{-sw}}$ varies from 0.73 to 1.38% (Fig. 8), though most shells have ranges around 1% (average for all shells = 1.04 \pm 0.25‰, 1 σ). Considering the limited seasonal range of SST in the study region during the study period (~4–6 °C) and limited seasonal range of SSS (\sim 0.1–2 psu) these adjusted range values are within expected ranges for bivalve δ^{18} O assuming a δ^{18} O_{sw} to SSS relationship of 0.27‰/psu for the Tropical Pacific (LeGrande and Schmidt, 2006; 2011). This approach is similar to fitting the $\delta^{18}O_{shell}$ to a SST record (e.g., Peharda et al., 2019) for time assignment except here we are fitting $\delta^{18}O_{sw}$ to the $\delta^{18}O_{shell}.$

4.2. Calibration of $\delta^{18}O_{shell}$ to SST

We use reduced major axis regression (RMA) with PAST 3.21 software (Hammer et al., 2001) with local monthly-averaged SST measurements from daily measurements at the Chimbote station (IMARPE, 2019; Fig. 2B) with the monthly *Donax obesulus* $\delta^{18}O_{shell}$ with $\delta^{18}O_{sw}$ removed ($\delta^{18}O_{sh-sw}$) to describe the relationship between $\delta^{18}O_{sh-sw}$ and SST. This regression technique is used because it includes bivariate uncertainty in both regressors (Thirumalai et al., 2011). Regression of average monthly $\delta^{18}O_{sh-sw}$ to monthly SST using all shells (Fig. 9) results in the following equation with a Root Mean Square Error (RSME) of $\pm 0.21\%$ or $1.01~^{\circ}C$.

$$\delta^{18}O_{\text{sh-sw}} = 3.18(\pm 0.14) - 0.20(\pm 0.01)\text{SST}, (n = 231)$$
 (6)

Table 2 Monthly $\delta^{18}O_{shell}$ summary without and with $\delta^{18}O_{sw}$ adjustment applied.

Shell	Year	$\begin{array}{c} Minimum \\ \delta^{18}O_{shell} \end{array}$	$\begin{array}{l} Minimum \\ \delta^{18}O_{sh\text{-sw}} \end{array}$	$_{\delta^{18}O_{shell}}^{Mean}$	$_{\delta^{18}O_{sh}}$	$\substack{\text{Median}\\ \delta^{18}O_{shell}}$	$\substack{\text{Median}\\ \delta^{18}O_{sh}.}$	$\begin{array}{l} Maximum \\ \delta^{18}O_{shell} \end{array}$	$\begin{array}{l} Maximum \\ \delta^{18}O_{sh\text{-sw}} \end{array}$	$\begin{array}{c} Range \\ \delta^{18}O_{shell} \end{array}$	Range $\delta^{18}O_{sh}$	SST range	n (months)
					sw		SW				sw	(°C)	
VBTB12-17	2012	-1.53	-1.51	-0.99	-0.88	-0.95	-0.87	-0.56	-0.51	0.97	1.00	4.55	15
VBTB12-25	2012	-1.34	-1.44	-1.02	-0.91	-1.12	-0.88	-0.27	-0.30	1.04	1.04	4.55	13
VBTB12-37	2012	-1.63	-1.31	-0.98	-0.81	-0.96	-0.81	-0.35	-0.37	1.28	0.85	4.55	14
VBTB12-118	2012	-1.55	-1.19	-1.25	-0.95	-1.23	-0.94	-0.99	-0.63	0.56	0.90	4.55	13
VBTB12-270	2012	-1.48	-1.02	-0.92	-0.78	-0.92	-0.80	-0.45	-0.36	1.04	0.88	4.55	18
VBTB12-360	2012	-1.36	-1.38	-0.87	-0.81	-0.97	-0.74	-0.38	-0.34	0.98	1.08	4.55	15
Mean		-1.48	-1.31	-1.01	-0.86	-1.03	-0.84	-0.50	-0.42	0.98	0.96	4.55	14.7
CMD14-8	2014	-1.36	-1.28	-1.01	-0.78	-0.98	-0.78	-0.75	-0.26	0.61	1.22	4.94	12
CMD14-123	2014	-1.59	-1.21	-1.07	-0.70	-1.13	-0.72	-0.62	-0.35	0.97	0.86	4.80	9
CMD14-129	2014	-1.56	-1.39	-1.07	-0.77	-1.02	-0.77	-0.52	-0.25	1.04	1.27	5.85	14
CMD14-134	2014	-1.79	-1.28	-1.27	-0.91	-1.25	-0.92	-0.79	-0.55	1.00	1.01	5.85	15
CMD14-142	2014	-1.27	-1.37	-1.03	-0.86	-1.04	-0.85	-0.61	-0.46	0.66	0.98	5.85	14
CMD14-144	2014	-1.66	-1.35	-1.10	-0.99	-1.07	-1.00	-0.56	-0.59	1.10	1.16	4.94	12
Mean		-1.54	-1.31	-1.09	-0.84	-1.08	-0.84	-0.64	-0.41	0.90	1.08	5.37	12.7
16AP-6	2016	-1.44	-1.84	-0.78	-1.04	-0.81	-1.04	-0.46	-0.46	0.98	1.38	5.63	13
16AP-26	2016	-1.14	-1.25	-0.64	-0.95	-0.62	-1.00	-0.45	-0.52	0.69	0.73	5.63	13
16AP-37	2016	-1.07	-1.36	-0.82	-1.05	-0.80	-1.06	-0.34	-0.34	0.73	1.02	5.63	13
16AP-51	2016	-1.21	-1.75	-0.85	-1.14	-0.84	-1.11	-0.68	-0.70	0.53	1.05	5.63	12
16AP-71	2016	-1.39	-1.64	-0.80	-1.14	-0.60	-1.20	-0.40	-0.51	0.99	1.13	5.63	9
16LC-168	2016	-0.90	-1.50	-0.32	-0.92	-0.19	-0.79	0.01	-0.29	0.91	1.21	5.63	7
Mean		-1.19	-1.56	-0.70	-1.04	-0.64	-1.03	-0.39	-0.47	0.81	1.09	5.63	11.2

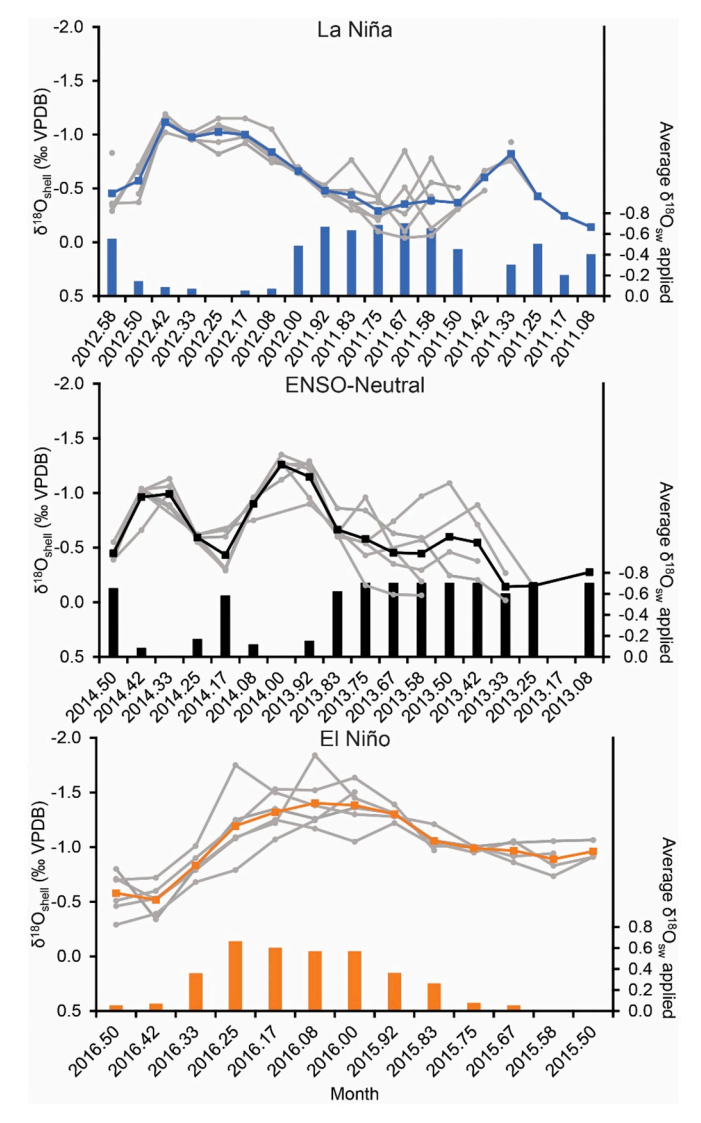


Fig. 8. Shell values with $\delta^{18}O_{sw}$ were subtracted as guided by residuals between our model and observed $\delta^{18}O_{shell}.$ The x-axis is the month represented by the subsample, the colored line is the average of all samples for that month and light gray lines are individual shell records. The secondary y-axis is the $\delta^{18}O_{sw}$ value applied to address the residual. The primary y-axis is inverted so that warmer values are up. The 2012 and 2014 secondary y-axes are also inverted.

La Niña (2012) and ENSO-neutral (2014) shells' monthly $\delta^{18}O_{sh\text{-sw}}$ generally overlap, though the overall range of 2014 monthly averages is slightly greater (Fig. 9). El Niño (2016) shells have overall more negative $\delta^{18}O_{sh\text{-sw}}$ monthly averages compared to the other years. When the influence of $\delta^{18}O_{sw}$ is removed, *Donax obesulus* $\delta^{18}O_{sh\text{-sw}}$ significantly correlates with SST ($r^2=0.76, p=0.001, \alpha=0.05$).

Given that we know the exact dates of shell collection, we can also examine the annual range of $\delta^{18}O_{shell}$ as a proxy for the annual range of SST. We compare the annual range (i.e., seasonal cycle) of SST measured at Chimbote (IMARPE, 2019) for each individual shell's lifespan with the calculated SST ranges from $\delta^{18}O_{shell}$ and $\delta^{18}O_{sh-sw}$ using our slope of $-0.20\%/^\circ\text{C}$ (Eq. 5; Table 3). Of our 18 unadjusted shells, 10 (55.6%) were within 1 °C of the expected SST range, and 11 (61.1%) were within 1.5 °C (or equivalent to the range of $\delta^{18}O_{sw}$). A total of 15 (83.3%) shells with adjustment for $\delta^{18}O_{sw}$ were within 1 °C, which increases to 17 (94.4%) shells if we loosen the criteria to 1.5 °C.

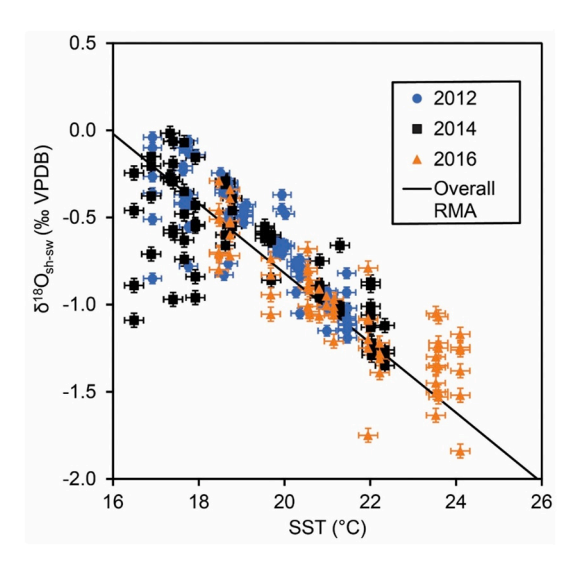


Fig. 9. Scatterplot of average monthly $\delta^{18}O_{sh\text{-sw}}$ for each study interval and Chimbote monthly SST (IMARPE, 2019) and linear regression fit determined using RMA. Error bars in both variables are their respective standard error of the mean.

4.3. Verification

We obtained data for $\delta^{18}O_{shell}$ of a *D. obesulus* specimen purchased live from a fish market in Huanchaco, Peru July 31, 2006 (Miguel Etayo-Cadavid, personal communication April 2021) by Etayo-Cadavid (2010). This shell was sampled using a smaller spatial resolution (0.08 mm) along the outside of the shell that had not been cross-sectioned or placed into epoxy. We thus consider it a good opportunity to test the fidelity of our method and Eq. 5 for *D. obesulus* sampled with a different method. Given the smaller drill bit, Etayo-Cadavid was able to obtain 100 individual measurements spanning the entire life of the specimen. Based on the von Bertalanffy growth equation for *D. obesulus* these measurements represent ~408 days in total. The 2006 shell's $\delta^{18}O$ ranges from -2.3 to 0.2%, with a distinct seasonal cycle (Fig. 10). Given that the shell lived through both ENSO-neutral and La Niña conditions, the minimum shell $\delta^{18}O$ values would translate into anomalously warm temperatures.

Applying Eq. 6 to the 2006 $\delta^{18}O_{shell}$, we estimate temperatures ranging from 15 to 27.5 $^{\circ}$ C. Unfortunately, IMARPE does not have data spanning 2005-2006 for Huanchaco as their monitoring of SST at that station did not begin until late 2008, but the nearest Optimum Interpolation Sea Surface Temperature (OISST) (Huang et al., 2021) 1° grid contains values ranging from 16.3–22.8 °C during the shell's life span. Given that the 2006 shell was sampled at what is likely sub-weekly resolution, and the OISST data are monthly average values, we averaged the $\delta^{18}O_{shell}$ values together in groups of seven to represent approximate monthly $\delta^{18}O_{shell}$. The resulting averaged values, when applied to Eq. 6, equate to SST ranging from 16.8–25.9 °C, or a reduction of 27% in range. Comparatively, the Carré et al. (2005) equation results in SST values ranging from 18.1-24.7 °C, and Grossman and Ku (1986) eq. 1 results in SST values from 22.6-30.5 °C. Importantly, as in our 2012-2016 sampled shells, there appears to be a breakdown in the δ¹⁸O_{shell}-SST relationship in the first winter of life, as all equations overestimate the SST for the 2005-2006 austral winter (Fig. 11) and underestimate the SST for the 2006-2007 austral winter. If seasonally varying $\delta^{18} O_{sw}$ values are applied, the estimated SST range from the 2006 shell becomes 16.7–22.9 $^{\circ}$ C, which considering an RMSE of 1 $^{\circ}$ C replicates the range of SST for the Huanchaco region almost exactly.

Table 3 Calculated SST ranges from unadjusted shells and shells adjusted by $\delta^{18} O_{sw}.$

Shell	Local SST range (°C)	δ ¹⁸ O _{shell} (°C)	δ ¹⁸ O _{sh-sw} (°C)	SST- δ ¹⁸ O _{shell} (°C)	SST-δ ¹⁸ O _{sh-sw} (°C)
VBTB12-17	4.55	4.85	5.00	-0.30	-0.45
VBTB12-25	4.55	5.20	5.20	-0.65	-0.65
VBTB12-37	4.55	6.40	4.25	-1.85	0.30
VBTB12-118	4.55	2.80	4.50	1.75	0.05
VBTB12-270	4.55	5.15	4.40	-0.65	0.15
VBTB12-360	4.55	4.90	5.40	-0.35	-0.85
CMD14-8	4.94	3.05	5.10	1.89	-1.16
CMD14-123	4.80	4.85	4.30	-0.05	0.50
CMD14-129	5.85	5.20	5.70	0.65	-0.5
CMD14-134	5.85	5.00	3.65	0.85	0.80
CMD14-142	5.85	3.30	4.55	2.55	0.95
CMD14-144	4.94	5.50	3.80	-0.56	-0.86
16AP-6	5.63	4.90	6.90	0.73	-1.27
16AP-26	5.63	3.45	3.65	2.18	1.98
16AP-37	5.63	3.65	5.10	1.98	0.53
16AP-51	5.63	2.65	5.25	2.98	0.38
16AP-71	5.63	4.95	5.65	0.68	-0.02
16LC-168	5.63	4.55	6.05	1.08	-0.42
Within ±1 °C				55.6%	83.3%
Within ±1.5 °C				61.1%	94.4%

Note: Local SST ranges determined from IMARPE (2019) for Chimbote for the sampled portion of each shell's lifespans determined by the growth model, which are approximately one seasonal cycle. Values highlighted in light gray are those within $\pm 1~^{\circ}\text{C}$ of the known SST range, whereas those highlighted in darker gray are within $\pm 1.5~^{\circ}\text{C}$.

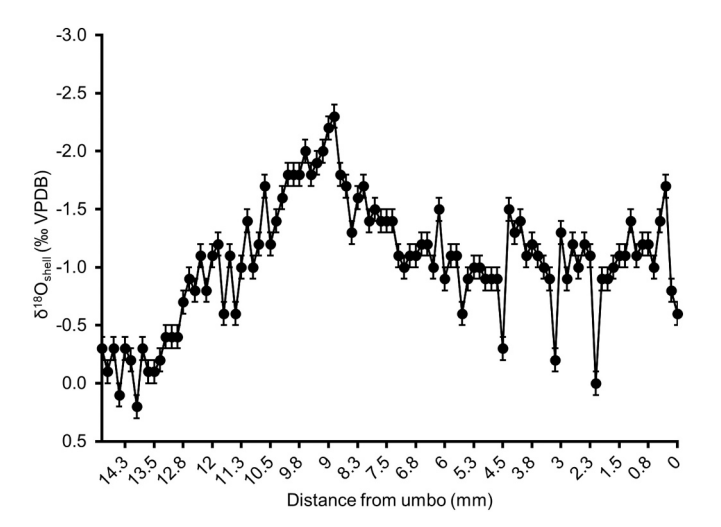


Fig. 10. 2006 *Donax obesulus* specimen $\delta^{18}O_{shell}$. Error bars are analytical precision ($\pm 0.1\%$, 1σ) reported by Etayo-Cadavid (2010). The direction of growth is right to left. The $\delta^{18}O$ axis is reversed so that warmer values are up.

4.4. Potential causes of anomalies in D. obesulus $\delta^{18}O_{shell}$

The overall shell mean values for ENSO-neutral and La Niña years follow the expected pattern associated with SST and SSS trends in

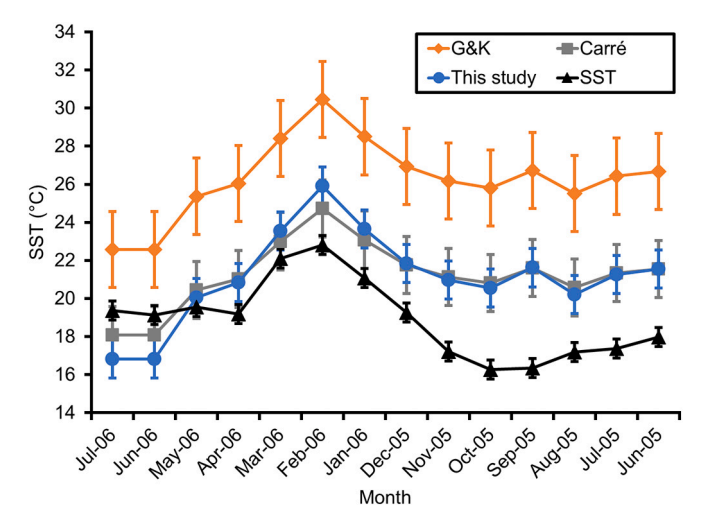


Fig. 11. Comparison of monthly average SST (black triangles) with monthly average calculated temperatures from the 2006 *Donax obesulus* specimen using three eqs. G + K = Grossman and Ku (1986), Carré = Carré et al., 2005. Error bars represent ± 0.5 °C for SST, an RMSE of ± 2 °C for Grossman and Ku (1986) based on our calculations, an estimated error of ± 1.5 °C for Carré et al., 2005 based on their calculations, and an RMSE of ± 1 °C for the equation developed in this study.

 $\delta^{18}O_{shell}$ (warmer-fresher conditions result in more negative values, colder-saltier conditions would be more positive), whereas the $\delta^{18}O$ in El Niño shells are anomalously higher. There are several possible explanations for this departure:

- 1. Shells are precipitated out of equilibrium with seawater.
- 2. Environmental stressors limited growth and thus truncated the $\delta^{18}{\rm O}$ signal in El Niño years.
- 3. Advection of open-water marine water masses into coastal areas introduced anomalous $\delta^{18} O_{sw}$ signals.
- 4. Other undetected hydrologic factors introducing anomalous $\delta^{18}O_{sw}$ signals (e.g., subsurface groundwater mixing with seawater, local evaporation effects).
- 5. Our sampling method could also have introduced some anomalies based on the small size of the shell compared to the diameter (0.5 mm) of the drill bit used.
- 6. The Carré equation is not representative of *D. obesulus* and different intercepts alongside different slopes are possible for different species thus explaining the offsets.

Oceanographic processes in our study area require careful consideration when interpreting D. obesulus $\delta^{18}O_{shell}$. El Niño and La Niña years do not always follow expected patterns of warm-wet and cold-dry conditions (Fig. 1). Moreover, we suggest caution as the SSS data we reference is a reanalysis product (Zuo et al., 2019) with a spatial resolution of $1^{\circ} \times 1^{\circ}$. Direct observations of SSS for coastal Peru are limited and thus reanalysis products may not accurately reflect the complex hydrology of coastal Peru. Our use of an extended range for $\delta^{18}O_{sw}$ in the far eastern Pacific is supported by Conroy et al. (2017), who found complex spatial and temporal trends in hydroclimate in the Galapagos that resulted in a $\delta^{18}O_{sw}$ range of -0.7 to 0.5%.

Contrary to previous work (Carstensen et al., 2010), we do not find evidence for La Niña cold events negatively influencing the life span of our shells or $\delta^{18}O_{shell}$ results (Table 2). The study of Carstensen et al. (2010) performed in vitro experiments using wild-caught specimens of D. obesulus transplanted into aquaria that were suitably modified to resemble typical ENSO phase (La Niña, ENSO-neutral, El Niño) temperatures for coastal Chile. That study found that *D. obesulus* populations experience statistically significant reductions in shell growth and mass mortality when subjected to La Niña-like temperature (14.9 \pm 0.3 (1 σ) °C), but no such reductions in growth or increases in mortality occurred during ENSO-neutral or El Niño-like temperatures (17.8 \pm 0.3 (1 σ) °C and 24.6 \pm 0.3 (1 σ) °C, respectively). It is worth noting that Carstensen et al. (2010) chose their temperatures to reflect conditions in northern Chile, which is the southernmost extent of D. obesulus under El Niño conditions (Tomicic, 1985). Temperatures at our study location are consistently warmer (2000–2016 annual average = 19.7 \pm 0.7 (1 σ) $^{\circ}$ C) and rarely fall below 16 °C. Therefore, D. obesulus populations in our study area do not experience sustained La Niña temperatures in the range tested by the study of Carstensen et al. (2010).

There are some anomalies within the aggregated shell group measurements, which include limited ranges of $\delta^{18}O_{shell}$ and positive $\delta^{18}O_{shell}$ values associated with warm SSTs. However, these anomalies most likely reflect a combination of biological growth limitations, local seawater dynamics, the influence of $\delta^{18}O_{sw}$ on the overall $\delta^{18}O_{shell}$ signal, and uncertainties in time models (i.e., the actual time span for each sample). Biological lower temperature limits on shell growth may bias the earlier part (first few months) of a shell record by reducing growth. Specifically, shells may only record warmer SSTs (i.e., above $15\ ^{\circ}\text{C}$ during austral winter of strong La Niña events) when individuals spawn in the austral spring or summer. Austral winter $\delta^{18}O_{sw}$ variability could result in a reduced SST signal in some cases (i.e., advection towards the coast in the early stages of El Niño events). Though measurements of seasonal cycles of $\delta^{18}O_{sw}$ are relatively limited along the coastline of Peru, they can include wide ranges (>0.5%, Grados et al., 2018), which can also act to enhance or suppress the reconstructed δ^{18} O-

SST range. Additionally, limited local SST observations from the same bay that our samples originate from (Paz and Alzamora, 2014) suggest that temperature can vary between the Anconcillo and Vesique beaches by up to 1.4 °C during the summer, or by as little as 0.4 °C during the winter. Such spatial variability in bay thermal dynamics could thus be the source of truncated signals from some of our La Niña and El Niño shells. For example, Bonicelli et al. (2014) found that in the southern portion of a small bay in Chile, which was sheltered from wind activity, diurnal temperature gradients were much lower than in the northern, less sheltered portion of the same bay. As our market purchased (2012, 2014) shells possibly came from a mixture of several beaches, truncated signals could thus represent areas of the bays that were more sheltered from temperature fluctuations driven by onshore winds earlier in the day. Similar temperature gradients and circulation patterns have been observed in other upwelling influenced bays worldwide (Largier, 2020).

Some shells indicate possible kinetic fractionation effects in positive correlations between $\delta^{18}O_{shell}$ and $\delta^{13}C_{shell}$ (McConnaughey and Gillikin, 2008), yet all the 2016 collected shells have more positive $\delta^{18}O_{shell}$ values relative to other years. Those shells that indicate possible kinetic fractionation effects also only do so for short intervals of shell growth, usually earlier in life (the first 1–3 months). We thus eliminate kinetic fractionation as the likely cause as there is no consistent evidence of kinetic fractionation in the 2016 shells or shells from other years. It is also likely that at least some of the environmental signals related to $\delta^{18}O_{shell}$ are truncated due to the biological growth limits of D. obesulus, but not to the extent that would be seen in these shells, as they were collected in an area where conditions are ideal for growth (i.e., SST rarely drops below 15 °C). Overall, correlations between models and shell data for 2016 are robust despite offsets.

When validating our paleotemperature equation using a D. obesulus shell collected in 2006 and sampled using a higher resolution, we found that our paleotemperature equation outperformed both the Carré et al. (2005) and Grossman and Ku (1986) equations in estimating minimum SST but overestimated maximum SST and thus SST range. However, all three equations overestimated maximum SST, and only the Carré et al. (2005a, 2005b) equation accurately predicted the range of SST, thus there appear to be other drivers of $\delta^{18}O_{shell}$ affecting our results. Crucially, as in our 2012-2016 sampled valves, there is an overestimation of SST in the first winter and summer of life, whether we use the averaged or reported values. There is also an underestimation of SST in the second winter. Thus, these offsets appear to be driven by local oceanography and/or shell biology rather than sampling methodology. With the underestimation of winter SSTs that would be near the biological limits of D. obesulus growth, we consider local oceanographic dynamics to be the most likely source of reconstructed temperature anomalies in the 2006 verification shell as well as our dataset.

We posit that the advection of open-ocean waters introducing anomalous $\delta^{18}O_{sw}$ values (option 3) is a likely scenario. Modeling and measurements of $\delta^{18} O_{sw}$ in the tropical eastern Pacific (LeGrande and Schmidt, 2006) suggest that open-ocean values range from 0 to 0.6%. We have received anecdotal reports from residents of the Nepeña coastline of oceanic flooding events during strong El Niños, with advected water reaching several hundred meters inland. Several studies (Muis et al., 2018; Peng et al., 2020; Piecuch and Quinn, 2016) support these accounts of anomalous sea level rise and coastal flooding associated with El Niño events. During El Niños, Ekman transport along the coastline of Peru weakens, Kelvin waves propagate across the ocean, and the water column expands allowing warmer, saltier ocean water to inundate coastal bays and their shorelines usually isolated by strong upwelling. The study of Morton et al. (2000) notes similar processes in barrier islands offshore of Colombia during El Niño events. Modeling and monitoring of zonal current anomalies also suggest that advection towards the coast happens during El Niño events (Espinoza-Morriberón et al., 2017).

4.5. D. obesulus $\delta^{18}O_{shell}$ as a paleoclimate proxy

Reconstructing SST values from individual $\it{D.obesulus}$ shells would require careful consideration of the potential influence of interannual and seasonally varying $\delta^{18}O_{sw}$. Our calibration considered seasonally varying $\delta^{18}O_{sw}$ within a range of 0.6% for each phase, which introduces anomalies equivalent to errors of $\pm 1.5~^{\circ}C$ ($\pm 0.3\%$) based on our calculated slope of $-0.20\%/^{\circ}C$. Given that our slope is similar to that calculated by Kim et al. (2007) for inorganically precipitated aragonite ($-0.20\%/^{\circ}C$) and is also close to the slopes calculated by Grossman and Ku (1986) for mollusks ($-0.21\%/^{\circ}C$) and various aragonitic calcifiers ($-0.23\%/^{\circ}C$), we consider it appropriate for $\it{D.obesulus}$. The difference in intercepts however leads to the mean shifts between reconstructed SST and observed SST, suggesting that equations developed for other species are likely not appropriate for $\it{D.obesulus}$.

Trace elemental ratios, specifically shell Ba/Ca, have been suggested as a method to reconstruct salinity or shifting water masses in bivalves (Gillikin et al., 2008; Hatch et al., 2013; Marali et al., 2017; Markulin et al., 2019; Poulain et al., 2015; Wanamaker and Gillikin, 2019). We have archived powders from our micromilling that can be used for future analysis that would allow us to examine Sr/Ca, Mg/Ca, and Ba/Ca from the same temporal resolution as our δ^{18} O results but these analyses are beyond the scope of this study. Although we have not yet examined whether shell Ba/Ca is a proxy for salinity in D. obesulus, the results presented in Izzo et al. (2017) are particularly encouraging and could lead to paired elemental and isotopic analyses in future studies. A paired proxy approach (trace elemental ratios and δ^{18} O) could allow for independent quantitative assessment of the influence of $\delta^{18}O_{sw}$ in individual shells (Bougeois et al., 2014; Gentry et al., 2008). However, there are still some questions regarding the fidelity of trace elements in mollusks as quantitative environmental proxies (Carré et al., 2006; Poulain et al., 2015; Surge and Lohmann, 2008; Surge and Walker, 2006; Wanamaker and Gillikin, 2019).

5. Conclusions

Peruvian *D. obesulus* $\delta^{18}O_{shell}$ shows promise as a temperature proxy capable of providing information on paleo-ENSO. ENSO phase influences both SST and $\delta^{18}O_{sw}$ at our study site, providing an opportunity to understand how signals change during ENSO events (i.e., SST and water mass changes occurring over weeks to months in specific temporal patterns). There are some limitations in the impact of wide (\sim 1‰), seasonal and ENSO phase variable ranges of $\delta^{18}O_{sw}$ on accurate SST reconstructions, especially given that applying $\delta^{18}O_{sw}$ values to address residuals between modeled and observed δ¹⁸O_{shell} require prior knowledge of local SST and time of shell collection. Additionally, whereas our growth models appear successful, there are still some questions regarding the potential error in time assignment within individual shells. Both limitations make the application of D. obesulus to paleotemperature reconstructions difficult but not impossible and are targets for future research. Understanding the dynamics of $\delta^{18}O_{sw}$ in the region should also be a goal not only for improving our results but any future attempts at developing other marine calcifiers' $\delta^{18}\text{O}$ signals as potential proxies for SST in the region.

Caveats aside, D. obesulus based reconstructions would provide new insights into past intervals when increased El Niño activity disrupted the biogeography of the colder water species M. donacium used in previous ENSO reconstructions. We posit that D. obesulus $\delta^{18}O_{\text{shell}}$ is a promising proxy that stands to provide more detail in the reconstructed history of paleoclimate variability along the north coast of Peru when used cautiously (i.e., from a population statistics standpoint akin to Carré et al. (2014) with M. donacium and when factors such as $\delta^{18}O_{\text{sw}}$ are constrained). We also posit that this method could be extended to Donax spp. in other regions. However, we caution that little information can likely be drawn from individual D. obesulus specimens, necessitating replication sampling strategies and robust statistical treatments to

reduce uncertainty in any reconstruction.

Software, samples, and data availability

Physical samples are in storage at the LSU PAST lab in Baton Rouge, LA, USA. Isotopic data associated with this article are archived at the World Data Service for Paleoclimatology www.ncdc.noaa.gov/data-access/paleoclimatology-data, 325 Broadway, Boulder, Colorado; IGBP PAGES/World Data Center for Paleoclimatology Data Contribution Series #TBA (Contribution # to be assigned before publication). The 2006 D. obesulus individual data is archived in Miguel Etayo-Cadavid's dissertation, available at https://ir.ua.edu/handle/123456789/912.

Declaration of Competing Interest

None

Acknowledgments

The authors are not aware of any affiliations, memberships, funding, or financial holdings that might be perceived as affecting the objectivity of this research. We would like to thank our funding sources, the National Science Foundation (Award #1805702), and the Department of the Interior South Central Climate Adaptation Science Center Cooperative Agreement G15AP00136 for supporting this research. We thank Chris Maupin, Alan Wanamaker, Becky H. Plaisance, and LSU's Paleoclimate and Anthropological Studies (PAST) lab student workers for their contributions to this project. We also thank Yofre Villa Real for his assistance in collecting specimens. We would also like to thank Donna Surge, an anonymous reviewer, and editor Michael E. Boettcher for their comments and suggestions.

Appendix A. Supplementary data

Supplementary data to this article can be found online at https://doi.org/10.1016/j.chemgeo.2021.120638.

References

- Arntz, W.E., Brey, T., Tarazona, J., Robles, A., 1987. Changes in the structure of a shallow sandy-beach community in Peru during an El Niño event. S. Afr. J. Mar. Sci. 5 (1), 645–658.
- Böhm, F., Joachimski, M.M., Dullo, W.-C., Eisenhauer, A., Lehnert, H., Reitner, J., Wörheide, G., 2000. Oxygen isotope fractionation in marine aragonite of coralline sponges. Geochim. Cosmochim. Acta 64 (10), 1695–1703. https://doi.org/10.1016/ S0016-7037(99)00408-1.
- Bonicelli, J., Moffat, C., Navarrete, S.A., Largier, J.L., Tapia, F.J., 2014. Spatial differences in thermal structure and variability within a small bay: Interplay of diurnal winds and tides. Cont. Shelf Res. 88, 72–80. https://doi.org/10.1016/j.csr.2014.07.009
- Bougeois, L., de Rafélis, M., Reichart, G.-J., de Nooijer, L.J., Nicollin, F., Dupont-Nivet, G., 2014. A high resolution study of trace elements and stable isotopes in oyster shells to estimate Central Asian Middle Eocene seasonality. Chem. Geol. 363, 200–212. https://doi.org/10.1016/j.chemgeo.2013.10.037.
- Buddemeier, R.W., Maragos, J.E., Knutson, D.W., 1974. Radiographic studies of reef coral exoskeletons: rates and patterns of coral growth. J. Exp. Mar. Biol. Ecol. 14, 179–200.
- Butler, P.G., Schöne, B.R., 2017. New research in the methods and applications of sclerochronology. Palaeogeogr. Palaeoclimatol. Palaeoecol. 465, 295–299.
- Butler, P.G., Wanamaker Jr., A.D., Scourse, J.D., Richardson, C.A., Reynolds, D.J., 2013. Variability of marine climate on the North Icelandic Shelf in a 1357-year proxy archive based on growth increments in the bivalve Arctica islandica. Palaeogeography Palaeoclimatolology Palaeoecology 373, 141–151. https://doi.org/10.1016/j.palaeo.2012.01.016.
- Carré, M., Bentaleb, I., Blamart, D., Ogle, N., Cardenas, F., Zevallos, S., Kalin, R.M., Ortlieb, L., Fontugne, M., 2005a. Stable isotopes and sclerochronology of the bivalve Mesodesma donacium: potential application to Peruvian paleoceanographic reconstructions. Palaeogeogr. Palaeoclimatol. Palaeoecol. 228 (1–2), 4–25. https:// doi.org/10.1016/j.palaeo.2005.03.045.
- Carré, M., Bentaleb, I., Bruguier, O., Ordinola, E., Barrett, N.T., Fontugne, M., 2006. Calcification rate influence on trace element concentrations in aragonitic bivalve shells: evidences and mechanisms. Geochim. Cosmochim. Acta 70 (19), 4906–4920. https://doi.org/10.1016/j.gca.2006.07.019.

- Carré, M., Bentaleb, I., Fontugne, M., Lavallee, D., 2005b. Strong El Niño events during the early Holocene: stable isotope evidence from Peruvian sea shells. Holocene 15 (1), 42–47. https://doi.org/10.1191/0959683605h1782rp.
- Carré, M., Klaric, L., Lavallée, D., Julien, M., Bentaleb, I., Fontugne, M., Kawka, O., 2009. Insights into early Holocene hunter-gatherer mobility on the Peruvian Southern Coast from mollusk gathering seasonality. J. Archaeol. Sci. 36 (5), 1173–1178. https://doi.org/10.1016/j.jas.2009.01.005.
- Carré, M., Sachs, J.P., Wallace, J.M., Favier, C., 2012a. Exploring errors in paleoclimate proxy reconstructions using Monte Carlo simulations: paleotemperature from mollusk and coral geochemistry. Clim. Past 8 (2), 433–450. https://doi.org/ 10.5194/cp-8-433-2012.
- Carré, M., Azzoug, M., Bentaleb, I., Chase, B.M., Fontugne, M., Jackson, D., Ledru, M.-P., Maldonado, A., Sachs, J.P., Schauer, A.J., 2012b. Mid-Holocene mean climate in the south eastern Pacific and its influence on South America. Quat. Int. 253, 55–66. https://doi.org/10.1016/j.quaint.2011.02.004.
- Carré, M., Sachs, J.P., Schauer, A.J., Rodríguez, W.E., Ramos, F.C., 2013. Reconstructing El Niño-Southern Oscillation activity and ocean temperature seasonality from shortlived marine mollusk shells from Peru. Palaeogeogr. Palaeoclimatol. Palaeoecol. 371, 45–53. https://doi.org/10.1016/j.palaeo.2012.12.014.
- Carré, M., Sachs, J.P., Purca, S., Schauer, A.J., Braconnot, P., Falcón, R.A., Julien, M., Lavallée, D., 2014. Holocene history of ENSO variance and asymmetry in the eastern tropical Pacific. Science 345 (6200), 1045–1048.
- Carstensen, D., 2010. Environmentally Induced Responses of *Donax Obesulus* and *Mesodesma donacium* (Bivalvia) Inhabiting the Humboldt Current System. Bremen University, Bremen, Germany. Doctoral Dissertation.
- Carstensen, D., Laudien, J., Leese, F., Arntz, W., Held, C., 2009. Genetic variability, shell and sperm morphology suggest that the surf clams *Donax marincovichi* and *D. obesulus* are one species. J. Molluscan Stud. 75 (4), 381–390. https://doi.org/ 10.1093/mollus/eyp036.
- Carstensen, D., Riascos, J.M., Heilmayer, O., Arntz, W.E., Laudien, J., 2010. Recurrent, thermally-induced shifts in species distribution range in the Humboldt current upwelling system. Mar. Environ. Res. 70 (3), 1–14.
- Chamberlayne, B.K., Tyler, J.J., Gillanders, B.M., 2021. Controls over oxygen isotope fractionation in the waters and bivalves (*Arthritica helms*) of an estuarine lagoon system. Geochem. Geophys. Geosyst. 22 https://doi.org/10.1029/2021GC009769 e2021GC009769.
- Chicoine, D., Rojas, C., 2012. Marine exploitation and paleoenvironment as viewed through molluscan resources at the early Horizon center of Huambacho, Nepeña Valley, Peru. Andean Past 10, 284–290.
- Chicoine, D., Rojas, C., 2013. Shellfish resources and maritime economy at Caylán, coastal Ancash, Peru. The Journal of Island and Coastal Archaeology 8 (3), 336–360. https://doi.org/10.1080/15564894.2013.787567.
- Coan, E.V., 1983. The Eastern Pacific Donacidae. Veliger 25 (4), 273-298.
- Conroy, J.L., Thompson, D.M., Cobb, K.M., Noone, D., Rea, S., LeGrande, A.N., 2017. Spatiotemporal variability in the δ^{18} O-salinity relationship of seawater across the tropical Pacific Ocean. Paleoceanography 32 (5), 484–497. https://doi.org/10.1002/2016PA003073.
- DeLong, K.L., Flannery, J.A., Maupin, C.R., Poore, R.Z., Quinn, T.M., 2011. A coral Sr/ca calibration and replication study of two massive corals from the Gulf of Mexico. Palaeogeogr. Palaeoclimatol. Palaeoecol. 307 (1), 117–128. https://doi.org/ 10.1016/j.palaeo.2011.05.005.
- Domínguez, N., Grados, C., Vásquez, L., Gutiérrez, D., Chaigneau, A., 2017. Climatología termohalina frente a las costas del Perú. Periodo: 1981–2010 Rep, 5–13 pp. Instituto del Mar del Peru (IMARPE).
- Epstein, S., Buchsbaum, R., Lowenstam, H.A., Urey, H.C., 1953. Revisted carbonatewater isotopic temperature scale. Bull. Geol. Soc. Am. 64, 1315–1325.
- Espinoza-Morriberón, D., Echevin, V., Colas, F., Tam, J., Ledesma, J., Vásquez, L., Graco, M., 2017. Impacts of El Niño events on the Peruvian upwelling system productivity. Journal of Geophysical Research: Oceans 122 (7), 5423–5444. https://doi.org/10.1002/2016jc012439.
- Etayo-Cadavid, M.F., 2010. Peruvian Mollusk Shells as Multi-Proxy Archives: Late Holocene Upwelling Variation and El Niño-Induced Biomineralization Effects on Trace Elements. The University of Alabama, Tuscaloosa, AL, USA. Doctoral Dissertation.
- Etayo-Cadavid, M.F., Andrus, C.F.T., Jones, K.B., Hodgins, G.W.L., Sandweiss, D.H., Uceda-Castillo, S., Quilter, J., 2013. Marine radiocarbon reservoir age variation in *Donax obesulus* shells from northern Peru: late Holocene evidence for extended El Niño. Geology 41 (5), 599–602.
- Etayo-Cadavid, M.F., Andrus, C.F.T., Jones, K.B., Hodgins, G.W.L., 2018. Subseasonal variations in marine reservoir age from pre-bomb *Donax obesulus* and *Protothaca asperrima* shell carbonate. Chem. Geol. https://doi.org/10.1016/j. chemgeo.2018.07.001.
- Galimberti, M., 2010. Investigation the Use of Oxygen and Carbon Isotopes and Sclerochronology on *Turbo Sarmaticus* and *Donax Serra* for Palaeoenvironment Reconstruction at Pinnacle Point, South Africa. University of Cape Town. Doctoral Dissertation
- Gentry, D.K., Sosdian, S., Grossman, E.L., Rosenthal, Y., Hicks, D., Lear, C.H., 2008. Stable isotope and Sr/ca profiles from the marine gastropod *Conus ermineus*: testing a multiproxy approach for inferring paleotemperature and paleosalinity. PALAIOS 23 (3/4), 195–209.
- Gillikin, D.P., Lorrain, A., Paulet, Y.-M., André, L., Dehairs, F., 2008. Synchronous barium peaks in high-resolution profiles of calcite and aragonite marine bivalve shells. Geo-Mar. Lett. 28 (5), 351–358. https://doi.org/10.1007/s00367-008-0111-9

Goodwin, D., Schöne, B.R., Dettman, D.L., 2003. Resolution and fidelity of oxygen isotopes as paleotemperature proxies in bivalve mollusk shells: models and observations. PALAIOS 18, 110–125.

- Grados, C., Chaigneau, A., Echevin, V., Dominguez, N., 2018. Upper Ocean hydrology of the Northern Humboldt Current System at seasonal, interannual and interdecadal scales. Prog. Oceanogr. 165, 123–144. https://doi.org/10.1016/j. pocean.2018.05.005.
- Gröcke, D.R., Gillikin, D., 2008. Advances in mollusc sclerochronology and sclerochemistry: tools for understanding climate and environment. Geo-Mar. Lett. 28, 265–268.
- Grossman, E.L., Ku, T.-L., 1986. Oxygen and carbon isotope fractionation in biogenic aragonite: temperature effects. Chemical Geology: Isotope Geoscience Section 59, 59–74. https://doi.org/10.1016/0168-9622(86)90057-6.
- Hallmann, N., Burchell, M., Schöne, B.R., Irvine, G.V., Maxwell, D., 2009. Highresolution sclerochronological analysis of the bivalve mollusk Saxidomus gigantea from Alaska and British Columbia: techniques for revealing environmental archives and archaeological seasonality. J. Archaeol. Sci. 36 (10), 2353–2364. https://doi. org/10.1016/j.jas.2009.06.018.
- Hammer, Ø., Harper, D.A.T., Ryan, P.D., 2001. PAST: Paleontological statistics software package for education and data analysis. Palaeontol. Electron. 4 (1). https://pal aeo-electronica.org/2001 1/past/issue1 01.htm.
- Hatch, M.B.A., Schellenberh, S.A., Carter, M.L., 2013. Ba/ca variations in the modern intertidal bean clam *Donax gouldii*: an upwelling proxy? Palaeogeogr. Palaeoclimatol. Palaeoecol. 373, 98–107.
- Huang, B., Liu, C., Banzon, V., Freeman, E., Graham, G., Hankins, B., Smith, T., Zhang, H.-M., 2021. Improvements of the Daily Optimum Interpolation Sea Surface Temperature (DOISST) Version 2.1. J. Clim. 34, 2923–2939. https://doi.org/ 10.1175/JCLI-D-20-0166.1.
- Hudson, J.H., Shinn, E.A., Halley, R.B., Lidz, B., 1976. Sclerochronology: a tool for interpreting past environments. Geology 4, 361–364.
- IMARPE, 2019. Temperatura superficial del mar y anomalías térmicas en el litoral peruano. www.imarpe.pe/imarpe/index.php?id_seccion=I0178030 200000000000000. Last Accessed: 12/30/2019.
- Izzo, C., Manetti, D., Doubleday, Z.A., Gillanders, B.M., 2017. Calibrating the element composition of *Donax deltoides* shells as a palaeo-salinity proxy. Palaeogeogr. Palaeoclimatol. Palaeoecol. 484, 89–96. https://doi.org/10.1016/j. palaeo.2016.11.038.
- Jew, N.P., Fitzpatrick, S.M., Sullivan, K.J., 2016. δ¹⁸O analysis of *Donax denticulatus*: evaluating a proxy for sea surface temperature and nearshore paleoenvironmental reconstructions for the northern Caribbean. J. Archaeol. Sci. Rep. 8, 216–223. https://doi.org/10.1016/j.jasrep.2016.06.018.
- Jones, D.S., 1983. Sclerochronology: Reading the record of the molluscan shell: annual growth increments in the shells of bivalve molluscs record marine climatic changes and reveal surprising longevity. American Scientist 71 (4), 384–391.
- Jones, D.S., Quitmyer, I.R., Andrus, C.F.T., 2005. Oxygen isotopic evidence for greater seasonality in Holocene shells of *Donax variabilis* from Florida. Palaeogeogr. Palaeoclimatol. Palaeoecol. 228 (1–2), 96–108. https://doi.org/10.1016/j. palaeo. 2005 03 046.
- Kim, S.-T., O'Neil, J.R., Hillaire-Marcel, C., Mucci, A., 2007. Oxygen isotope fractionation between synthetic aragonite and water: Influence of temperature and Mg²⁺ concentration. Geochim. Cosmochim. Acta 71 (19), 4704–4715. https://doi. org/10.1016/j.gca.2007.04.019.
- Largier, J.L., 2020. Upwelling Bays: how Coastal Upwelling Controls Circulation, Habitat, and Productivity in Bays. Annu. Rev. Mar. Sci. 12 (1), 415–447. https://doi. org/10.1146/annurev-marine-010419-011020.
- Lavado-Casimiro, W., Espinoza, J.C., 2014. Impacts of El Niño and La Niña in the precipitation over Peru. Revista Brasiliera de Meterologia 29 (2), 171–182. https:// doi.org/10.1590/S0102-77862014000200003.
- LeGrande, A.N., Schmidt, G.A., 2006. Global gridded data set of the oxygen isotopic composition in seawater. Geophys. Res. Lett. 33 (12) https://doi.org/10.1029/2006-0126011
- LeGrande, A.N., Schmidt, G.A., 2011. Water isotopologues as a quantitative paleosalinity proxy. Paleoceanogr. Paleoclimatol. 26 (3) https://doi.org/10.1029/ 2010PA002043.
- Locarnini, R.A., Mishonov, A.V., Antonov, J.I., Boyer, T.P., Garcia, H.E., Baranova, O.K., Zweng, M.M., Johnson, D.R., 2010. World Ocean Atlas 2009, volume 1: Temperature. S. Levitus, Ed. NOAA Atlas NESDIS 68. U.S. Government Printing Office, Washington, D.C, 184 pp.
- Marali, S., Schöne, B.R., Mertz-Kraus, R., Griffin, S.M., Wanamaker, A.D., Matras, U., Butler, P.G., 2017. Ba/ca ratios in shells of Arctica islandica—potential environmental proxy and crossdating tool. Palaeogeogr. Palaeoclimatol. Palaeoecol. 465, 347–361. https://doi.org/10.1016/j.palaeo.2015.12.018.
- Markulin, K., Peharda, M., Mertz-Kraus, R., Schöne, B.R., Uvanović, H., Kovač, Ž., Janeković, I., 2019. Trace and minor element records in aragonitic bivalve shells as environmental proxies. Chem. Geol. 507, 120–133. https://doi.org/10.1016/j. chemgeo.2019.01.008.
- McConnaughey, T.A., Gillikin, D.P., 2008. Carbon isotopes in mollusk shell carbonates. Geo-Mar. Lett. 28 (5), 287–299. https://doi.org/10.1007/s00367-008-0116-4.
- Mook, W.G., Vogel, J.C., 1968. Isotopic Equilibrium between Shells and their Environment. Science 159 (3817), 874–875. https://doi.org/10.1126/ science.159.3817.874.
- Morton, R., Gonzalez, J., Correa, I., López, G., 2000. Frequent Non-storm Washover of Barrier Islands, Pacific Coast of Colombia. J. Coast. Res. 16, 82–87.
- Muis, S., Haigh, I.D., Guimarães Nobre, G., Aerts, J.C.J.H., Ward, P.J., 2018. Influence of El Niño-Southern Oscillation on Global Coastal Flooding. Earth's Future 6 (9), 1311–1322. https://doi.org/10.1029/2018ef000909.

- NOAA, 2020. Cold & Warm Episodes by Season Oceanic Niño Index (ONI), v5, edited.
 National Weather Service Climate Prediction Center.
- Palmer, K.L., Moss, D.K., Surge, D., Turek, S., 2021. Life history patterns of modern and fossil *Mercenaria* spp. from warm vs. cold climates. Palaeogeogr. Palaeoclimatol. Palaeoecol. 566. https://doi.org/10.1016/j.palaeo.2021.110227.
- Paredes, C., Cardoso, F., 2001. El Género *Donax* en la Costa Peruana (Bivalvia: Tellinoidea). Rev. Peru. Biol. 8 (2), 83–93.
- Paz, P.B., Alzamora, R.U., 2014. Sinopsis Biológico-Pesquera de la Marucha *Donax obesulus* Reeve, 1854 en el litoral de Ancash (Bahia Samanco), 2001-2009. Informe del Instituto del Mar del Perú 41 (1–4), 179–196.
- Paz, P.B., Aguilar, A.T., Nolazco, V.G., 2007. Población de "Marucha" Donax marincovichi (Coan, 1983) en Bahía Samanco, Región Áncash, Perú. Invierno 2006. Informe del Instituto del Mar del Perú 4 (2), 131–146.
- Peharda, M., Thébault, J., Markulin, K., Schone, B.R., Janekovic, I., Chauvaud, L., 2019. Contrasting shell growth strategies in two Mediterranean bivalves revealed by oxygen-isotope ratio geochemistry: the case of *Pecten jacobaeus* and *Glycymeris pilosa*. Chem. Geol. 526, 23–35. https://doi.org/10.1016/j.chemgeo.2017.09.029.
- Peng, Q., Xie, S.-P., Wang, D., Kamae, Y., Zhang, H., Hu, S., Zheng, X.-T., Wang, W., 2020. Eastern Pacific wind effect on the evolution of El Niño: implications for ENSO diversity. J. Climate 33 (8), 3197–3212. https://doi.org/10.1175/JCLI-D-19-0435.1.
- Perrier, C., Hillaire-Marcel, C., Ortlieb, L., 1994. Paléogéographie littorale et enregistrement isotopique (13C, 18O) d'événements de type El Niño par les mollusques holocènes et récents du nord-ouest péruvien. Géog. Phys. Quatern. 48 (1), 23–38. https://doi.org/10.7202/032970ar.
- Piecuch, C.G., Quinn, K.J., 2016. El Niño, La Niña, and the global sea level budget. Ocean Science 12 (6), 1165–1177. https://doi.org/10.5194/os-12-1165-2016.
- Poulain, C., Gillikin, D.P., Thébault, J., Munaron, J.M., Bohn, M., Robert, R., Paulet, Y. M., Lorrain, A., 2015. An evaluation of Mg/Ca, Sr/Ca, and Ba/ca ratios as environmental proxies in aragonite bivalve shells. Chem. Geol. 396, 42–50. https://doi.org/10.1016/j.chem.geo.2014.12.019.
- Ramírez, P., De La Cruz, J., Carbajal, W., 2016. *Donax obesulus*: Bioecología y Dinámica Poblacional en el Litoral de Lambayeque. Perú, Informe del Instituto del Mar del Perú 43 (2), 210–228.
- Reynolds, D.J., Butler, P.G., Williams, S.M., Scourse, J.D., Richardson, C.A., Wanamaker Jr., A.D., et al., 2013. A multiproxy reconstruction of Hebridean (NW Scotland) spring sea surface temperatures between AD 1805 and 2010. Palaeogeogr. Palaeoclimatol. Palaeoecol. 386, 275–285. https://doi.org/10.1016/j. palaeo.2013.05.029.
- Riascos, J., Carstensen, D., Laudien, J., Arntz, W., Oliva, M.E., Güntner, A., Heilmayer, O., 2008. Thriving and Declining: Temperature and Salinity Shaping Life-History and Population Stability of Mesodesma donacium in the Humboldt Upwelling System. In: CENSOR Endterm Symposium, 9–11 September 2008, Lima, Peru edited.
- Riascos, J.M., Heilmayer, O., Oliva, M.E., Laudien, J., 2011. Environmental stress and parasitism as drivers of population dynamics of *Mesodesma donacium* at its northern biogeographic range. ICES J. Mar. Sci. 68 (5), 823–833. https://doi.org/10.1093/ icesims/fsr026.
- Roberts, L.R., Holmes, J.A., Leng, M.J., Sloane, H.J., Horne, D.J., 2018. Effects of cleaning methods upon preservation of stable isotopes and trace elements in shells of *Cyprideis torosa* (Crustacea, Ostracoda): Implications for palaeoenvironmental reconstruction. Quat. Sci. Rev. 189, 197–209. https://doi.org/10.1016/j. quascirev.2018.03.030.
- Roselló, E., Vásquez, V.F., Morales, A., Rosales, T.E., 2001. Marine resources from an urban Moche (470–600 ad) area in the 'Huacas del Sol y de la Luna' archaeological complex (Truiillo, Peru). Int. J. Osteoarchaeol. 11, 72–87.
- Royer, C., Thébault, J., Chauvaud, L., Olivier, F., 2013. Structural analysis and paleoenvironmental potential of dog cockle shells (*Glycymeris glycymeris*) in Brittany, Northwest France. Palaeogeogr. Palaeoclimatol. Palaeoecol. 373, 123–132. https://doi.org/10.1016/j.palaeo.2012.01.033.
- Sandweiss, D.H., 2003. Terminal Pleistocene through Mid-Holocene archaeological sites as paleoclimatic archives for the Peruvian coast. Palaeogeogr. Palaeoclimatol. Palaeoecol. 194 (1–3), 23–40. https://doi.org/10.1016/S0031-0182(03)00270-0.
- Sandweiss, D.H., Kelley, A.R., 2012. Archaeological contributions to climate change research: the archaeological record as a paleoclimatic and paleoenvironmental archive. Ann. Rev. Anthropol. 41 (1), 371–391. https://doi.org/10.1146/annurevanthro-092611-145941.
- Sandwess, D.H., Maasch, K.A., Burger, R.L., Richardson III, J.B., Rollins, H.B., Clement, A., 2001. Variation in Holocene El Niño frequencies: climate records and cultural consequences in ancient Peru. Geology 29 (7), 603–606. https://doi.org/ 10.1130/0091-7613(2001)029<-0603:VHENO>.2.0.CO:2.
- Schöne, B.R., 2003. A 'clam-ring' master-chronology constructed from a short-lived bivalve mollusc from the northern Gulf of California, USA. The Holocene 13 (1), 39–49. https://doi.org/10.1191/0959683603hl593rp.

- Schöne, B.R., 2008. The curse of physiology challenges and opportunities in the interpretation of geochemical data from mollusk shells. Geo-Mar. Lett. 28, 269–285.
- Schöne, B., Gillikin, D., 2013. Unraveling environmental histories from skeletal diaries advances in sclerochronology. Palaeogeogr. Palaeoclimatol. Palaeoccol. 373, 1–5.
- Schöne, B.R., Surge, D., 2014. Bivalve shells: ultra highresolution paleoclimate archives. Past Global Changes Magazine 22, 20–21.
- Schöne, B.R., Oschmann, W., Rössler, J., Castro, A.D.F., Houk, S.D., Kröncke, I., et al., 2003. North Atlantic Oscillation dynamics recorded in shells of a long-lived bivalve mollusk. Geology 31, 1037–1040. https://doi.org/10.1130/G20013.1.
- Schöne, B.R., Pfeiffer, M., Pohlmann, T., Siegismund, F., 2005. A seasonally resolved bottom-water temperature record for the period AD 1866–2002 based on shells of *Arctica islandica* (Mollusca, North Sea). Int. J. Climatol. 25 (7), 947–962. https://doi. org/10.1002/joc.1174.
- Schöne, B.R., Wanamaker Jr., A.D., Fiebig, J., Thébault, J., Kreutz, K., 2011. Annually resolved 8 ¹³Cshell chronologies of long-lived bivalve mollusks (*Arctica islandica*) reveal oceanic carbon dynamics in the temperate North Atlantic during recent centuries. Palaeogeogr. Palaeoclimatol. Palaeoecol. 302, 31–42. https://doi.org/10.1016/j.palaeo.2010.02.002.
- Steinhardt, J., Butler, P.G., Carroll, M.L., Hartley, J., 2016. The Application of Long-Lived Bivalve Sclerochronology in Environmental Baseline monitoring. Front. Mar. Sci. 3, 176.
- Surge, D., Lohmann, K.C., 2008. Evaluating Mg/Ca ratios as a temperature proxy in the estuarine oyster, *Crassostrea virginica*. Journal of Geophysical Research: Biogeosciences 113, G02001. https://doi.org/10.1029/2007JG000623.
- Surge, D., Walker, K.J., 2006. Geochemical variation in microstructural shell layers of the southern quahog (*Mercenaria campechiensis*): implications for reconstructing seasonality. Palaeogeogr. Palaeoclimatol. Palaeoecol. 237 (2–4), 182–190.
- Talledo, C., 1980. Algunas consideraciones bioecologicas de *Donax peruvianus* Deshayes 1855. Tesis para optar el titulo de licenciado. Universidad Nacional Pedro Ruiz Gallo, Lambayeque, Peru, pp. 1–41.
- Tarifeño-Silva, E., 1980. Studies on the Biology of the Surf Clam Mesodesma donacium (Lamarck, 1818) (Bivalvia: Mesodesmatidae) from Chilean Sandy Beaches. University of California, Los Angeles, Los Angeles (CA. Doctoral Dissertation).
- Thirumalai, K., Partin, J.W., Jackson, C.S., Quinn, T.M., 2013. Statistical constraints on El Niño southern oscillation reconstructions using individual foraminifera: a sensitivity analysis. Paleoceanogr. Paleoclimatol. 28 (3), 401–412. https://doi.org/ 10.1002/palo.20037.
- Thirumalai, K., Singh, A., Ramesh, R., 2011. A MATLABTM code to perform weighted linear regression with (correlated or uncorrelated) errors in bivariate data. J. Geol. Soc. India 77 (4), 377–380. https://doi.org/10.1007/s12594-011-0044-1.
- Thompson, D.M., Ault, T.R., Evans, M.N., Cole, J.E., Emile-Geay, J., 2011. Comparison of observed and simulated tropical climate trends using a forward model of coral 8¹⁸O. Geophys. Res. Lett. 38 (14) https://doi.org/10.1029/2011g1048224.
- Tomicic, J., 1985. Efectos del fenómeno El Niño 1982–83 en las comunidades litorales de la península de Mejillones*Rep.*, 209–213 pp. Instituto Fomento Pesquero-Chile.
- Twaddle, R.W., Ulm, S., Hinton, J., Wurster, C.M., Bird, M.I., 2016. Sclerochronological analysis of archaeological mollusc assemblages: methods, applications and future prospects. Archaeol. Anthropol. Sci. 8, 359–379. https://doi.org/10.1007/s12520-015-0228-5.
- Tynan, S., Dutton, A., Eggins, S., Opdyke, B., 2014. Oxygen isotope records of the Australian flat oyster (*Ostrea angasi*) as a potential temperature archive. Mar. Geol. 357, 195–209. https://doi.org/10.1016/j.margeo.2014.07.009.
- von Bertalanffy, L., 1957. Quantitative Laws in Metabolism and growth. Q. Rev. Biol. 32 (3), 217–231. https://doi.org/10.1086/401873.
- Waite, A.J., Swart, P.R., 2015. The inversion of aragonite to calcite during the sampling of skeletal archives: Implications for proxy interpretation. Rapid Commun. Mass Spectrom. 29 (10), 955–964. https://doi.org/10.1002/rcm.7180.
- Wanamaker, A.D., Gillikin, D.P., 2019. Strontium, magnesium, and barium incorporation in aragonitic shells of juvenile Arctica islandica: Insights from temperature controlled experiments. Chem. Geol. 526, 117–129. https://doi.org/10.1016/j. chemeeo.2018.02.012.
- White, R.M.P., Dennis, P.F., Atkinson, T.C., 1999. Experimental calibration and field investigation of the oxygen isotopic fractionation between biogenic aragonite and water. Rapid Commun. Mass Spectrom. 13 (13), 1242–1247. https://doi.org/ 10.1002/(sici)1097-0231(19990715)13:13<1242::\did-rcm627>3.0.Co;2-f.
- Zuo, H., Balmaseda, M.A., Tietsche, S., Mogensen, K., Mayer, M., 2019. The ECMWF operational ensemble reanalysis-analysis system for ocean and sea ice: a description of the system and assessment. Ocean Sci. 15 (3), 779–808. https://doi.org/10.5194/os-15-779-2019.